UC San Diego

UC San Diego Electronic Theses and Dissertations

Title

Modeling Perspective of the Physical-Biological Response of the California Current to ENSO

Permalink

https://escholarship.org/uc/item/22t2r3rb

Author

Cordero Quiros, Nathali

Publication Date

2020

Peer reviewed|Thesis/dissertation

eScholarship.org Powered by the California Digital Library
University of California

UNIVERSITY OF CALIFORNIA SAN DIEGO

Modeling Perspective of the Physical-Biological Response of the California Current to ENSO

A dissertation submitted in partial satisfaction of the requirements for the degree
Doctor of Philosophy

in

Oceanography

by

Nathalí Cordero Quirós

Committee in charge:

Arthur J. Miller, Chair
Christopher Edwards
Peter J.S. Franks
Sarah N. Giddings
Francesco Lanza Di Scalea
Aneesh C. Subramanian

2020

Copyright

Nathalí Cordero Quirós, 2020

All rights reserved.

The dissertation of Nathalí Cordero Quirós is approved, and it is acceptable in quality and form for publication on microfilm and electronically:

_____

_____

_____

_____

_____

_____

_____

Chair

University of California San Diego

2020

DEDICATION

I am lucky enough to be surrounded by a lot of especial people who filled my journey with adventures and love.

Thank you, God, the one who lives in me, the one who lives in you. For always leading me to the places I belong.nThank you, Mamá, Papá, and (not so little now) Brother. Thank you not just to my mom, but to Linda, my friend, my guide, my eternal hero.

To my first mentor in Mexico, Juan Carlos, for feeding my curiosity and motivating my journey into oceanography, always helping me to dive more deeply into it. Even when you'll never forgive me for taking the physics path. Paula, thank you for all of your guidance, support, and inspiration while being my mentor, until today. Thank you both for always believing that I could go further.

To my mentor, Art Miller, to lovely Jenny, and Team Miller… Thank you for making me feel at home. To the different generations of Team Miller, thank you for being so amazing, Manu, Aneesh, Dillon, Mike, Jonathan, Osi, Mer, Momme, Tash, Dani, and Liz. Thank you, Art, for all the hard work, for being a mentor, and a friend. For inspiring me to grow, not only in science, but in life too.

Thank you, Alejandra, Raquel, Eduardo, and Johnny, my international family. Gracias Alejandra for all those chats in the kitchen at your place, and for looking after me.

Patty, thank you for all the good moments, the unconditional friendship, and for being my partner in crime. To my old-time friends Gerardo, Netox, Alicia, Ileana, Jimena, Sandy, and Yury, for showing me the true meaning of friendship, for always being there for me.

To my favorite brazilians, Dani and Leticia, for being like sisters to me. For all the discussions about science and life. For showing me that friendship can grow from diversity and not only from similarities. To all the beautiful women that I've met along this journey, some of whom I mentioned already. Jenny, Tashiana, Liz, Margherita, Antonietta, Mer, Raphäelle, Laura, Erica, Cristal, Vale. I've learned so much from you, thank you for showing me the magic of finding strength in softness. I always carry you in my heart. And of course, there cannot be balance without a pinch of masculinity… Thank you, Alfredo, Gabo, Lorenzo, Arturo, Tiago, for all the laughs, and for the serious conversations too. Thank you, Simo for all the good memories, and all the especial people found along the way, Dario R., Alexis, Marco, Frank, Ernesto, Ana, Ari, Marce, Jona, Dario. Thanks for filling my journey with a good dose of fun.

TABLE OF CONTENTS

LIST OF FIGURES

LIST OF TABLES

ACKNOWLEDGEMENTS

I want to thank Dr. Arthur J. Miller for his guidance, support, and hours spent helping me to refine this thesis.

Chapter 2, in full, is a reprint of the material as it appears in Ocean Modelling 2019 Cordero-Quirós, N., Miller, A.J., Subramanian A.C., Luo, J.Y., Capotondi, A., 2019. Composite physical-biological El Niño and La Niña conditions in the California Current System in CESM1-POP2-BEC. Ocean Modelling, 142, 101439. https://doi.org/10.1016/j.ocemod.2019.101439. The dissertation author was the primary investigator and author of this paper.

The model simulation (ROMS-NEMURO) used for this research was executed and generously provided by Dr. Enrique Curchitser and Dr. Raphael Dussin (Department of Environmental Sciences, Institute of Marine and Coastal Sciences, Rutgers University). The work presented in this chapter was facilitated by two CCE-LTER REU's from UCSD, Ms. Yunchun Pan (Applied Mathematics) and Mr. Lawrence Balitaan (Oceanic and Atmospheric Science). The results of Chapter 3 are currently being prepared for submission for publication, by Nathalí Cordero-Quirós, Arthur J. Miller, Yunchun Pan, Lawrence Balitaan, Raphael Dussin, and Enrique Curchitser. I also acknowledge Dr. Jerome Fiechter at University of California, Santa Cruz, for this helpful feedback and guidance in understanding the IBM. Prof. Chris Edwards provided extensive advice on the NEMURO model.

I thank the members of the committee for their feedback and help in finishing this dissertation. We are grateful to the National Science Foundation (California Current Ecosystem-LTER, OCE1637632, and Coastal SEES, OCE1600283) and the National Oceanic and Atmospheric Administration (NOAA-MAPP; NA17OAR4310106) for funding that supported this research. N. Cordero-Quirós was partially supported by a UC Mexus CONACYT Fellowship.

VITA

2012	B.S. in Oceanology Autonomous University of Baja California, Ensenada, Mexico
2011-12	Research Assistant Ensenada Center for Scientific Research and Higher Education, Mexico
2015	M.S. in Physical Oceanography Ensenada Center for Scientific Research and Higher Education, Mexico
2015-20	Graduate Research Assistant Scripps Institution of Oceanography University of California San Diego
2020	Ph.D. in Oceanography Scripps Institution of Oceanography University of California San Diego

PUBLICATIONS

Cordero-Quirós, N., Miller, A.J., Subramanian A.C., Luo, J.Y., Capotondi, A., 2019. Composite physical-biological El Niño and La Niña conditions in the California Current System in CESM1-POP2-BEC. Ocean Modelling, 142, 101439. https://doi.org/10.1016/j.ocemod.2019.101439

Cordero-Quirós, N., Miller, A. J., Pan, Y., Balitaan, L., Dussin, R., and Curchitser, E., 2020: Physical-ecological response of the California Current System to ENSO events in ROMS-NEMURO. In preparation.

FELLOWSHIPS

UC MEXUS-CONACYT

ABSTRACT OF THE DISSERTATION

Modeling Perspective of the Physical-Biological Response of the California Current to ENSO

by

Nathalí Cordero Quirós

Doctor of Philosophy in Oceanography

University of California San Diego, 2020

Arthur J. Miller, Chair

The California Current System (CCS) is one of the most productive regions in the whole world, and as such, one of the most studied as well. Observational records throughout the years have shown scientists that CCS is under the influence of major climate events such as El Niño Southern Oscillation (ENSO). Yet there are still many questions regarding the exact mechanisms trough which ENSO teleconnections imprint variability in the physical conditions of the CCS, and how this further impacts the California Current Ecosystem (CCE).

The focus of this dissertation is to shed light over the regional expressions of ENSO over the CCS, and how physical-biogeochemical interactions drive a coherent response associated with El Niño and La Niña events. The first part describes the response of the CCS to ENSO as

captured by one coarse resolution model and one eddy-resolving high-resolution model. The findings help to better understand the mechanistic response of the CCS to ENSO and build on the existing framework for ecosystem predictability. A key result from the first part is that the cooling of the CCS associated with La Niña is more consistent than the warming associated with El Niño. Also, with the high-resolution model we are able to show the bottom-up response of the CCE, and the diversity in the response among different trophic groups.

The last part focuses on proposing new avenues for future research to untangle the intricate components of the CCE response that are associated with mesoscale activity, and how they are affected by ENSO variability.

Chapter 1

1.1 Introduction

The California Current System (CCS) supports a productive ecosystem because it is one of the world's Eastern Boundary Upwelling Systems (EBUS; e.g., Bakun et al., 2015). These are characterized by upwelling-favorable winds that intensify during the local spring season, setting up an environment for high primary production along the coast (Hickey, 1998). As cool, salty and high-nutrient waters are upwelled to the photic zone, populations of phytoplankton and zooplankton bloom, starting the production from the bottom of the trophic chain up to the higher levels represented by fish and other top predators (e.g., McClatchie, 2014).

The dynamics of the California Current Ecosystem (CCE) are highly dependent upon the physical conditions (e.g., Checkley and Barth, 2009). Thus, variables like sea surface temperature (SST), thermocline depth, surface heat fluxes, horizontal currents, and the intensity of the upwelling act as the physical drivers of the ecosystem. The variability of the CCS is under the influence of major climate events, such as the El Niño Southern Oscillation (ENSO), which modifies these ecosystem drivers (e.g., Di Lorenzo et al., 2013a). This physical variability usually peaks during wintertime, synchronous with ENSO atmospheric and oceanic teleconnections, and potential predictability arises from this oscillatory environmental behavior (e.g., Alexander et al., 2002). Many previous studies have addressed the response of the CCE to forcings by ENSO but each event seems to produce unique surprises in the local response, both in the physics and in the ecology (e.g., Jacox et al., 2015). In addition, questions regarding the practical usefulness of ENSO predictability in the context of the CCE still remain unanswered (e.g., Jacox et al., 2020). Ocean models with physical, biogeochemical (BGC), and ecological

components can both provide us with excellent tools to complement observations and help us to shed light on CCS ecosystem dynamics as a response to ENSO and other climate events (e.g., Franks et al., 2013; Miller et al., 2015).

One of the basic ways that we think about the response of the ecosystem to physical climate forcing is through bottom-up changes that are driven by variability of ocean upwelling, which might then lead to an ecological response that is linearly related to the intensity of the physical climate forcing (e.g., Di Lorenzo et al., 2013b). The ecological response, in turn, can include components that are intrinsic to the ecology that may be unrelated to the environmental forcing (e.g., Edwards et al., 2000). Sorting out the ecological response in the context of these two factors is at the heart of quantifying how predictable the ecosystem might be. The situation is further complicated by the nonlinear behavior of the ocean, which includes mesoscale eddy processes, turbulent mixing, and lateral advection, as well as random midlatitude weather variability. Since the natural environment is relatively coarsely sampled in time and space (e.g., Capotondi et al., 2019), using simulations of the physical-biological response to climate forcing can help us better understand the way the system might behave in the real world.

Global climate models now include representations of ecology and biogeochemistry that attempt to simulate the current climate and can be used to project future climate changes and associated BGC and ecological responses (e.g., Hurrell et al., 2012). However, these models have relatively coarse resolution and may not be capable of representing EBUS processes such as those that occur in the CCS and CCE (e.g., Stock et al., 2011). Highly resolved regional ocean models, forced at the boundary by either observations or coarse-resolution models, provide a

means to better represent coastal upwelling, mesoscale eddy evolution, biogeochemical transport, and coastal geometry and bathymetry, on the ecological response (e.g., Curchitser et al., 2013). But the eddy field from those types of models is random so that the local response cannot be directly compared to observations. In addition, the eddies constitute noise when trying to isolate the ENSO-forced part of the physical and ecological response. Because of this, it is challenging to separate the part of the ecosystem response that is related to changes in the eddy field, which has limited predictability on weekly to monthly time scales, and the part forced by climate variability, which may have predictability on seasonal to interannual time scales (e.g., Di Lorenzo and Miller, 2017).

In this dissertation, I take a careful look at both a coarse-resolution "climate-scale" global ocean model and a high-resolution "eddy-scale" regional ocean model to assess the impact of observed ENSO-scale forcing on the regional ecological response in the California Current. The climate model analysis was motivated by the desire of the CCE-LTER to collaboratively develop an ecological model with NCAR scientists that contains all the fundamental elements considered essential by CCE biologists (e.g., Ohman et al., 2013; Franks et al., 2013). **Chapter 2** (Cordero-Quirós et al., 2019) is the result of my analysis of the basic physical-biological global ocean model (~1 deg resolution) used by NCAR in the CESM (Community Earth System Model), namely POP2 (Parallel Ocean Program version 2) coupled to the ecosystem model BEC (Biogeochemical Elemental Cycling).

After diagnosing the robust signals of ENSO in the regional response of the "climate-scale" model, I recognized its many deficiencies. I subsequently established a collaboration with

Rutgers scientists who had a high-resolution physical-biological CCS simulation readily available for analysis. **Chapter 3** (Cordero-Quirós et al., 2020) is the result of that study, which uses a (~7km resolution) ROMS (Regional Ocean Modeling System) simulation in the CCS with NEMURO (North Pacific Ecosystem Model for Understanding Regional Oceanography) and a particle-tracking IBM (Individual Based Model) for small pelagic fish. Although this run lacks the BGC component of POP2, it includes more sophisticated planktonic components as well as the higher trophic level populations of sardine and anchovy. This system allows us to neatly show bottom-up ENSO-driven changes within the different plankton communities and to establish food-predator relationships between them. This work was facilitated by two CCE-LTER REU's from UCSD, Ms. Yunchun "Pauline" Pan (Applied Mathematics) and Mr. Lawrence "Rence" Balitaan (Oceanic and Atmospheric Science), whom I mentored during summer 2019 by teaching them techniques of statistical analysis and numerical model evaluation.

Overall, this dissertation builds on the existing framework for ecosystem predictability derived from the regional expressions of ENSO over the CCS (Jacox et al., 2020; Capotondi et al., 2019). Instead of focusing on individual ENSO events or assuming a bimodal distribution for Eastern Pacific versus Central Pacific ENSO events (see Capotondi et al., 2015), I focus here on extracting a response of the CCS that is coherent through all warm or cold events associated with ENSO. Composites of physical and ecosystem variables are constructed by averaging El Niño and La Niña years to obtain 'typical' conditions of the CCS during ENSO events (cf., Turi et al., 2018). The spread of the histograms around those composite gives a measure of skill reliability for the model system, which is compared with available observations.

One key feature that I found in my analysis of both models is the surprising asymmetry in the physical response of the CCS to ENSO. Cold La Niña events are more consistently cold than warm El Niño events are consistently warm, even though the most extreme events are the warm ones. The origins of this local asymmetry, which is also observed in nature, appear to be due to similar asymmetries in the western tropical Pacific where the teleconnections to the Pacific-North America (PNA) pattern are forced during ENSO events.

Understanding the types of mechanistic responses of lower and higher trophic levels under a changing climate, such as I have studied here, is key for developing better short-term climate predictions of ecological response and habitat changes that can be exploited by managers of fisheries in establishing quotas. In addition, the knowledge that I have gained can be used to help policy makers plan for long-term changes of the CCS as global warming conditions continue to amplify and affect the coastal economics of U.S. West Coast fisheries.

With these practical issues in mind, **Chapter 4** both summarizes the main results of my research and also considers the limits of ecosystem predictability by proposing avenues for future research. I discuss ways to use models to assess how sensitive an ecosystem model might be to slight changes in the physical forcing. This is important because we can never know the physical environment perfectly so that small errors in physics might cascade into large errors in ecology. I also explain ways to use models to assess the importance of "high-frequency" mesoscale eddy variability on the slowly evolving climate-scale response. The ecological response to these eddies might generate enhanced incoherent signals (noise) or consistent eddy-

driven structures locked to slowly varying geographic features. Ensembles of these types of ecological simulations provide a way forward to continue to untangle the complicated features of the predictable parts of ecological response to physical forcing from the fundamentally chaotic components of both climate dynamics and the ecosystem itself.

References

Alexander, M.A., Bladé, I., Newman, M., Lanzante, J.R., Lau, N.C., Scott, J.D., 2002. The atmospheric bridge: The influence of ENSO teleconnections on air-sea interaction over the global oceans. J. Clim. 15, 2205–2231.

Capotondi, A., Wittenberg, A.T., Newman, M., Di Lorenzo, E., Yu, J.-Y., Braconnot, P., Cole, J., DeWitte, B., Giese, B., Guilyardi, E., Jin, F.-F., Karnauskas, K., Kirtman, B., Lee, T., Schneider, N., Xue, Y., Yeh, S.-W., 2015. Understanding ENSO diversity. Bull. Amer. Meteorol. Soc. 96, 921–938.

Capotondi, A., Jacox, M., Bowler, C., Kavanaugh, M., Lehodey, P., Barrie, D., Brodie, S., Chaffron, S., Cheng, W., Faggiani Dias, D., Eveillard, D., Guidi, L., Iudicone, D., Lovenduski, N., Nye, J. A., Ortiz, I., Pirhalla, D. E., Pozo Buil, M., Saba, V., Sheridan, S. C., Siedlecki, S., Subramanian, A., De Vargas, C., Di Lorenzo, E., Doney, S.C., Hermann, A. J., Joyce, T., Merrifield, M., Miller, A. J., Not, F., Pesant, S. 2019: Observational needs supporting marine ecosystems modeling and forecasting: From the global ocean to regional and coastal systems. Frontiers in Marine Science, 6, 623.

Checkley, D.M., Barth,J.A., 2009. Patterns and processes in the California Current System. Prog.Oceanogr.84,49–64. Doi: https://doi.org/10.1016/j.pocean.2009.07.028

Cordero-Quirós, N., Miller, A.J., Subramanian A.C., Luo, J.Y., Capotondi, A., 2019. Composite physical-biological El Niño and La Niña conditions in the California Current System in CESM1-POP2-BEC. Ocean Modelling, 142, 101439. https://doi.org/10.1016/j.ocemod.2019.101439EN Curchitser, E.N., HP Batchelder, H.P., DB Haidvogel, D.B., Fiechter, J., Runge, J. 2013. Advances in physical, biological, and coupled ocean models during the US GLOBEC program. Oceanography 26 (4), 52-67. DOI 10.5670/oceanog.2013.75

Di Lorenzo, E., Combes, V., Keister, J.E., Strub, P.T., Thomas, A.C., Franks, P.J.S., Ohman, M.D., Furtado, J.C., Bracco, A., Bograd, S.J., Peterson, W.T., Schwing, F.B., Chiba, S., Taguchi, B., Hormazabal, S., Parada, C., 2013. Synthesis of Pacific Ocean climate and ecosystem dynamics. Oceanography 26, 68–81.

Di Lorenzo, E., D. Mountain, H. P. Batchelder, N. Bond and E. E. Hofmann, 2013: Advances in Marine Ecosystem Dynamics from US GLOBEC The Horizontal-Advection Bottom-up Forcing Paradigm. Oceanography, 26(4) 22-33, doi:10.5670/oceanog.2013.73.

Di Lorenzo, E., Miller, A.J., 2017. A framework for ENSO predictability of marine ecosystem drivers along the US West Coast. US CLIVAR Variations 15, 1–7.

Edwards, C. A., Powell, T.A., Batchelder, H.P. 2000: The stability of an NPZ model subject to realistic levels of vertical mixing. J. Mar. Res., 58, 37–60.

Franks, P.J.S., DiLorenzo, E., Goebel, N.L., Chenillat, F., Riviere, P., Edwards, C.A., Miller, A.J., 2013. Modeling physical–biological responses to climate change in the California Current System. Oceanography26,26–33.

Hickey, B.M., 1998. Coastal oceanography of western North America from the tip of Baja California to Vancouver Island. In: Robinson, A.R., Brink, K.H. (Eds.), The Sea, The Global Coastal Ocean: Regional Studies and Syntheses. J. Wiley and Sons Inc, New York, pp. 345–391.

Hurrell, J.W., Holland, M.M., Gent, P.R., Ghan, S., Kay, J.E., Kushner, P.J., Marque, J.-F., Large, W.G., Lawrence, D., Lindsay, K., Lipscomb, M.C., Mahowald, N., Marsh, D.R., Neale, R.B., Rasch, P., Vavrus, S., Vertenstein, M., Bader, D., Collings, W.D., Hack, J.J., Kiehl, J., Marshall, S., 2012. The community earth system model: A framework for colaborative research. Bull. Am. Meteorol. Soc. 94, 1339–1360. http://dx.doi.org/10.1175/BAMS-D-12-00121.1.

Jacox, M.G., Fiechter, J., Moore, A.M., Edwards, C.A., 2015. ENSO and the California Current coastal upwelling response. J. Geophys. Res. Oceans 120, 1691–1702.

Jacox, M.G., Alexander, M. A., Siedlecki, S., Chen, K., Kwon, Y.-O., Brodie, S., Ortiz, I., Tommasi, D., Widlansky, M. J., Barrie, D., Capotondi, A., Cheng, W., Di Lorenzo, E., Edwards, C., Fiechter, J., Fratantoni, P., Hazen, E. L., Hermann, A. J., Kumar, A., Miller, A. J., Pirhalla, D., Pozo Buil, M., Ray, S., Sheridan, S. C., Subramanian, A., Thompson, P., Thorne, L., Annamalai, H., Bograd, S. J., Griffis, R. B., Kim, H., Mariotti, A., Merrifield, M., and Rykaczewski, R. 2020: Seasonal-to-interannual prediction of North American coastal marine ecosystems: Forecast methods, mechanisms of predictability, and priority developments. Progress in Oceanography, 183, 102307.

McClatchie, S., 2014. Regional Fisheries Oceanography of the California Current System, The CalCOFI Program. Springer Netherlands. 10.1007/978-94-007-7223-6

Miller, A.J., Song, H., Subramanian, A.C., 2015. The physical oceanographic environment during the CCE-LTER Years: Changes in climate and concepts. Deep-Sea Res. 112, 6–17.

Ohman, M. D., K. Barbeau, P. J. S. Franks, R. Goericke, M. D. Landry and A. J. Miller, 2013: Ecological transitions in a coastal upwelling ecosystem. Oceanography, 26, 210-219

Stock, C.A., Alexander, M.A., Bond, N.A., Brander, K.M., 2011. On the use of IPCC-class models to assess the impact of climate on living marine resources. Prog. Oceanogr. 88, 1–27. https://doi.org/10.1016/j.pocean.2010.09.001.

Turi, G., Alexander, M., Lovenduski, N., Capotondi, A., Scott, J., Stock, C., Dunne, J., John, J., and Jacox, M., 2018. Response of Oxygen and PH to ENSO of the California Current System in a high-resolution global climate model. Ocean Sci., 14, 69-86.

Chapter 2

A composite physical-biological ENSO in the California Current System in CESM1-POP2-BEC

Nathali Cordero-Quirós[1], Arthur J. Miller[1], Aneesh C. Subramanian,[2] and Jessica Y. Luo [3].

[1] Scripps Institution of Oceanography, University of California, San Diego

[2] University of Colorado, Boulder, CO

[3] Climate and Global Dynamics, National Center for Atmospheric Research (NCAR), Boulder CO

Corresponding author: Scripps Institution of Oceanography, University of California, San Diego, La Jolla, CA 92093, USA.

Nathali Cordero-Quirós, nacorder@ucsd.edu

Abstract

El Niño-Southern Oscillation (ENSO) is recognized as one of the potentially predictable drivers of California Current System (CCS) variability. In this study, we analyze a 67-year coarse-resolution (~1°) simulation using the ocean model CESM-POP2-BEC forced by NCEP/NCAR reanalysis winds to develop a model composite of the physical-biological response of the CCS during ENSO events. The model results are also compared with available observations. The composite anomalies for sea surface temperature (SST), pycnocline depth, 0m-

100m vertically averaged chlorophyll, 0m-100m vertically averaged zooplankton, 25m-100m vertically averaged nitrate, and oxygen at 200m depth exhibit large-scale coherent relationships between physics and the ecosystem, including reduced nutrient and plankton concentrations during El Niño, and increased nutrient and plankton concentrations during La Niña. However, the anomalous model response in temperature, chlorophyll, and zooplankton is generally much weaker than observed and includes a 1-2 month delay compared to observations. We also highlight the asymmetry in the model CCS response, where composite model La Niña events are stronger and more significant than model El Niño events, which is a feature previously identified in observations of CCS SST as well as in tropical Pacific Niño-4 SST where atmospheric teleconnections associated with ENSO are forced. These physical-biological composites provide a view of some of the limitations to the potentially predictable impacts of ENSO teleconnections on the CCS within the modeling framework of CESM-POP2-BEC.

Keywords: ENSO, California Current System, composite, physical-biological interactions

2.1 Introduction

The California Current System (CCS) is among the most biologically productive oceanic regions of the world (*e.g.,* Hickey, 1998; Checkley and Barth, 2009; Miller *et al.,* 2015). The configuration of the wind patterns along this Eastern Boundary Upwelling System (EBUS) favors the existence of a large upwelling region that extends from northern Baja California, Mexico, to Oregon and Washington on the U.S. West Coast (*e.g.,* Bakun *et al.,* 2015). This phenomenon establishes the environment as a highly productive region that is subject to local variability, some of which is imprinted by atmospheric and oceanic teleconnections from remote

changes in the equatorial Pacific. One of the main physical drivers of CCS interannual variability is the El Niño-Southern Oscillation (ENSO), producing changes in sea surface temperature (SST), upwelling, lateral advection of water masses, pycnocline depth, surface heat flux, freshwater flux, eddy kinetic energy, and other fields. All these variables are known to be forcing agents for ecological conditions and biogeochemical content that affect the state of the ecosystem on ENSO time scales (*e.g.,* Schwing *et al.,*2005).

There are two main mechanisms by which ENSO drives changes in the CCS. The first (local atmospheric variability due to atmospheric teleconnections) is related to the intensification of the Aleutian Low (and associated weakening of the North Pacific High) that enhances poleward flow of warm air along the northeastern Pacific (Niebauer, 1988; Jacox *et al.,* 2015) and suppresses upwelling favorable winds along California coast. The second mechanism (oceanic variability due to remotely driven waves) is related to the equatorial Kelvin-like waves in the tropical ocean excited by the westerly winds and coupled ocean-atmosphere feedbacks during El Niño (McPhaden *et al.,* 1998). These waves propagate eastward across the Equatorial Pacific, and then poleward after colliding with the coast of South America (Chávez *et al.,* 2002). They are also potentially generated along the Central American and Baja California coasts by subtropical wind fields altered by the tropical ocean conditions. The remotely-driven wave mechanism also deepens the thermocline and suppresses upwelling of nutrient-rich waters both in the equatorial region and along the North American West Coast (*e.g.,* Frischknecht *et al.,* 2015). The combination of local atmospheric and remote oceanic variability imprinted by ENSO in the CCS plays an important role in understanding the CCS response during these events.

ENSO is known to have predictable components, some of which may significantly impact the CCS and therefore be exploitable for practical predictions (*e.g.,* Jacox *et al.,* 2017). While the effects of El Niño over land in the U.S. are well documented (Gershunov and Barnett, 1998; McPhaden et al. 1998; Wang *et al.,* 2012), its effects over the ocean are less understood, particularly because of limited observations. The CCS is unique because it is one of the most extensively sampled ocean regions (*e.g.,* Bograd and Lynn, 2002; Crawford *et al.,* 2017), with the California Cooperative Oceanic Fisheries Investigations (CalCOFI) providing hydrographic *in-situ* data since the late 1950s, along with various satellite measurements covering the area since the late 1970s. There are many studies that address the ecological effects of particular El Niño events over the CCS (*e.g.,* Bograd and Lynn, 2001; Chávez *et al.,* 2002; Jacox et al., 2016; Ohman, 2018) using the limited observations that indicate reduction of nutrient and plankton concentrations during warm conditions and vice versa for cold events. However, because of the sparseness of the data in both space and time, there is limited understanding of how consistently these warm and cold ENSO events impact both the physical and biological state of this region (*e.g.,* Di Lorenzo and Miller, 2017, summarize the results of a recent workshop on this topic).

Coupled physical and biogeochemical models represent an important tool for addressing oceanic variability and provide an alternative and complementary approach to using only direct observations for the study of marine ecosystems (*e.g.,* Curchitser *et al.,* 2013; Frischknecht *et al.,* 2015, 2017; Turi *et al.,* 2018). Analyzing the effects of ENSO on the CCS over the entire observational record in conjunction with model simulations may help to quantify how consistently the ENSO events impact the physical and biological system. This can also shed light

on how well model forecasts of ENSO variability might be trusted for developing useful outlooks for ecosystem resource management.

In this study, we analyze a 67-year-long physical-biogeochemical simulation driven by observed surface forcing using the oceanic component of the Community Earth System Model (CESM) to study the changes associated with El Niño and La Niña over the CCS. We first characterize the model's anomalous CCS ENSO response as a whole and then develop monthly-mean El Niño and La Niña composites (*cf.,* Turi *et al.,* 2018) for various physical and biogeochemical variables. After comparing the results with available observations, we identify the limitations that can be expected in both the physical and biological regional response to ENSO events, given observed atmospheric forcing and a coarse-resolution ocean model. Although the resolution of this model is coarse, it simultaneously includes the effects of physics, low trophic level ecology, and biogeochemistry, which together provide a large-scale synergistic perspective on the response compared to what can be assessed with simpler biological models or with observations alone. This model-analysis approach allows us to better illustrate the limited predictability of the physical-biological behavior of the CCS during ENSO events (*e.g.,* Ohman *et al.,* 2013; Franks *et al.,* 2013).

2.2 Data and Methods

2.2.1 Model

We employ a 67-year (1949-2015) hindcast simulation with 1° resolution and global coverage from the Community Earth System Model version 1 (CESM1; Hurrell *et al.,* 2013).

The ocean component is the Parallel Ocean Program, version 2 (POP2; Danabasoglu *et al.,* 2012), and the sea ice component is the Community Ice Code, version 4 (CICE4; Jahn *et al.,* 2014). The ocean biogeochemistry is based on the Biogeochemical Elemental Cycling (BEC; Moore *et al.,* 2002, 2004, 2013) model embedded in POP2. The ocean and ice components are forced by atmospheric reanalysis data, following the Coordinate Ocean-Ice Reference Experiments II (CORE2; Large and Yeager 2009) protocol that uses winds from the NCEP-NCAR reanalysis, except for the tropical band (30°S-30°N) that uses 20th Century Reanalysis (20CRv2) (Griffies *et al.,* 2009; Yeager *et al.,* 2018). Monthly means of all variables were available to be used in our subsequent analysis.

The ecosystem component consists of three explicit phytoplankton functional types, representing diatoms, diazotrophs, and small phytoplankton, with coccolithophores included as an implicit fraction of the latter, plus one zooplankton group. It also includes dynamic Carbon:Chlorophyll ratios and photoadaptation (Geider *et al.* 1997, 1998) as well as light and multiple nutrient (N, P, Si, Fe) co-limitation. BEC simulates the elemental cycles of nitrogen, phosphate, silicate, and iron, leading to skillful representations of oceanic chlorophyll, nutrients, and oxygen over the global ocean (Moore *et al*. 2002, 2004, 2013).

2.2.2 Observational data

Model validation for sea surface temperature anomalies (SSTa) was made using observations from the Hadley Centre Ice-Sea Surface Temperature (HadISST, Rayner *et al.,* 2003) from January 1949 to December 2015. The model SSTa are also compared over a single point at La Jolla, CA, using observations from the Shore Stations Program

(http://scripps.ucsd.edu/programs/shorestations/shore-stations-data/) during three different El Niño Events. The skewness of ENSO over the CCS is analyzed qualitatively using probability density functions (PDF) of SSTa derived from the modeled fields over the whole period (1949-2015) and SSTa from the HadISST for the same years.

Observed chlorophyll data was obtained from the Sea-viewing Wide Field-of-view-Sensor (SeaWiFS) Level 3 standard mapped image (SMI), with a monthly temporal resolution and 9.2 km resolution (O'Reilly *et al.,* 2000). We used chlorophyll from 1998 to 2010 to compare with the model response for that same period. The model chlorophyll fields were averaged down to a depth of 25 m as a proxy to compare with satellite surface chlorophyll concentration that measures over the local oceanic optical depth.

2.2.3 Methods

The hindcast simulation covers the time period January, 1949, to December, 2015. To focus on ENSO-related time scales, we eliminated the strong signals in the CCS associated with decadal (and longer, including trends) variability from the model fields and the observations. We used a Lanczos high-pass filter with a cutoff frequency of 10 years (following Turi *et al.,* 2018), which successfully removed the low-frequency energy in each variable for both model and observations.

All composite variables were constructed by averaging together each of the selected El Niño and La Niña events identified in the period of the simulation over the 3 months before and the 8 months after (i.e., a 12-month composite) the wintertime (DJF) peak of the event. The years identified as El Niño and La Niña follow the NOAA protocol

(NCEP/NOAA,http://origin.cpc.ncep.noaa.gov/products/analysis_monitoring/ensostuff/ONI_v5.php), but only include the moderate-to-strong events and exclude the weak events. In brief, we identify El Niño years as those when Niño-3.4 3-month averaged SSTa ≥1.0 °C and La Niña years as those when SSTa ≤-1.0 °C, where the anomalies persist during both the fall (SON) and winter (DJF) seasons. The resulting El Niño years included in the 12-month composite are: *1951-1952, 1957-1958, 1963-1964, 1965-1966, 1968-1969, 1972-1973, 1982-1983, 1986-1987, 1987-1988, 1991-1992, 1994-1995, 1997-1998, 2002-2003,* and *2009-2010*. The resulting years for the La Niña composite are: *1949-1950, 1955-1956, 1970-1971, 1971-1972, 1973-1974, 1975-1976, 1983-1984, 1984-1985, 1988-1989, 1995-1996, 1998-1999, 1999-2000, 2007-2008, 2010-2011,* and *2011-2012.* This yields a total of 14 El Niño events and 15 La Niña events.

Additional validation of SST fields was made via Empirical Orthogonal Function (EOF) analysis of the SSTa over the CCS. EOF1 from the model (including all months together) and its associated principal component (PC1) were compared to the first observed mode from HadISST and correlated with monthly values of NOAA's Climate Prediction Center (CPC) Oceanic Niño Index (ONI). For the composite results presented below, a total chlorophyll estimate (mg m^{-3}) was calculated as the sum of all three phytoplankton groups, averaged over the top 100 m of the water column to include any potential subsurface chlorophyll maximum. The same method was applied for zooplankton carbon biomass in mmol m^{-3}. Nutrient composites are represented by nitrate concentrations (mmol m^{-3}) averaged between 25m and 100m depth, corresponding to the strong vertical gradient in the nitracline. We also compute composite dissolved oxygen concentration (mmol m^{-3}) at a single depth of 200 m. The analysis was made over the CCS region extending from 21° N to 48° N, and from the coast to 132° W.

Anomalies were calculated by subtracting the 12-month climatology from the entire record after high-pass filtering. The 14 El Niño and 15 La Niña years as indicated by the SSTa were used to build the composite anomalies for SST, pycnocline depth (using the σ=26 isopycnal surface as a proxy), vertically averaged zooplankton biomass, vertically averaged chlorophyll concentrations, vertically averaged [NO_3], and [O_2] at 200m depth, which represent key indicators of both physical drivers and ecosystem state. The composites were tested for significance via bootstrap analysis as follows: a hundred composites were randomly computed for each variable and then compared to the composites of El Niño and La Niña obtained from the model. Only those anomalies greater than 2 standard deviations (2σ) of the random distribution are considered to be statistically significant at above the 95% level.

2.3. Results

2.3.1 Model validation with SST

As a broad-scale depiction of the overall interannual response of the CCS to the prescribed forcing, Fig. 2.1 shows the first mode (EOF1) of the SSTa over CCS calculated from the whole record of the model (left panel) and HadISST (right panel), with a 65.6% and a 63.6% of variance explained, respectively. EOF1 in the model dominates the coastal region from southern Baja California to Oregon, showing the coherency between these two regions, but extends further offshore than in observations. EOF1 from HadISST dominates over central and south Baja California, and it is coherent along Baja California and the California coast. Both in model and observations, the first mode of SSTa resembles the well-known pattern developed during warming related to El Niño along the CCS.

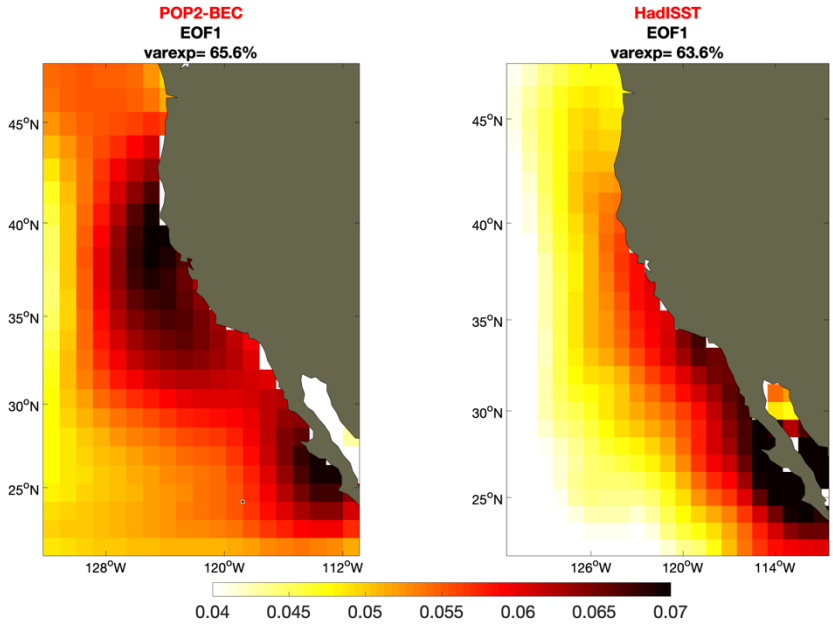

Figure 2.1 EOF1 calculated from the full record (1949-2015) of SSTa over CCS. Left panel shows EOF from model POP2-BEC; right panel shows observed EOF1 from HadISST.

The principal components (PC1) associated with the first modes are shown in Fig. 2.2 (top and middle). The PC1 of the model SSTa is well correlated (0.94) with PC1 from HadISST and they are both moderately correlated with the CPC-ONI (Fig. 2.2, bottom) with coefficients of 0.5 (HadISST) and 0.43 (model), indicating their relevance as the local imprint of ENSO teleconnections from the tropics.

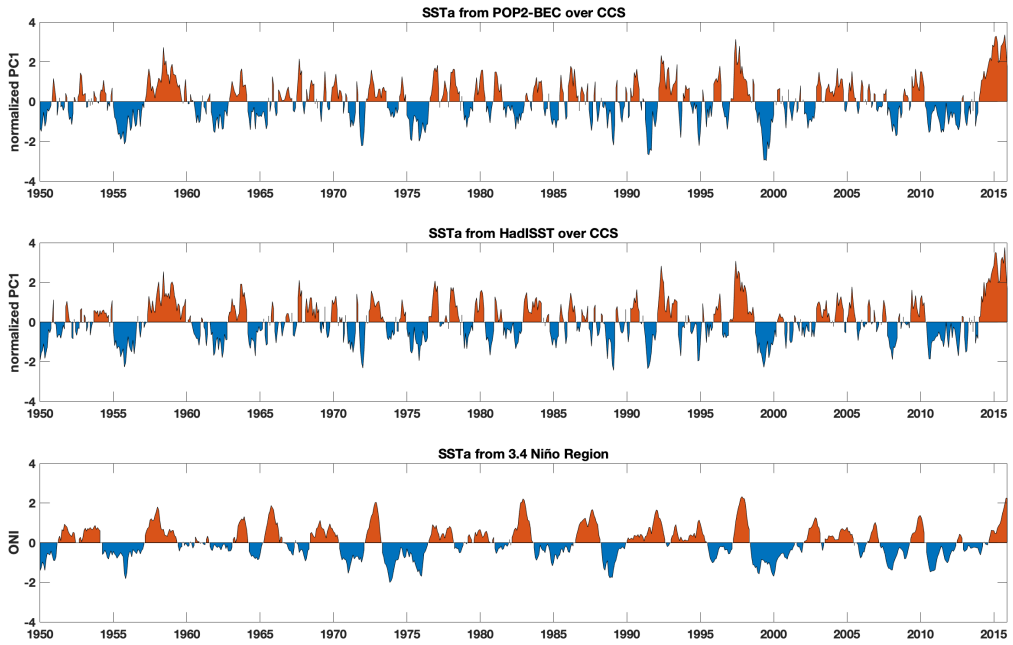

Figure 2.2 Normalized principal component (PC1) associated to the first mode of SSTa over CCS; a-b) model and observations, respectively. Observed NOAA's CPC ONI is shown in panel c) for comparison.

Another broad perspective on the performance of the model in representing interannual CCS variability is the monthly SSTa (°C) averaged over the CCS region for both the model and observations (Fig. 2.3, top). The correlation between these time series is 0.93, and the RMSE is 0.24, indicating a good agreement in both the timing and magnitude of the variability when averaged over the whole region. However, the model produces a somewhat weaker local response than observed when compared over a single point, which will become more apparent in subsequent analyses. For example, Fig. 2.3 (bottom) also shows the monthly SSTa from the model and from the Shore Stations Program at La Jolla/Scripps Pier station. Three of the strongest registered El Niño events are shown (1972-1973, 1982-1983 and 1997-1998), each one showing the year before and the year after the wintertime peak (DJF) of El Niño to compare the development and demise of these major events. The model only captures part of the variability of

the El Niño events in the CCS as indicated by the correlations of 0.70, 0.68, 0.78, respectively. The magnitude of the anomalies is also underestimated for these three major events at this location. The coarse model resolution, possible errors in surface forcing, and errors in model physical formulations limit the model performance in these pointwise evaluations.

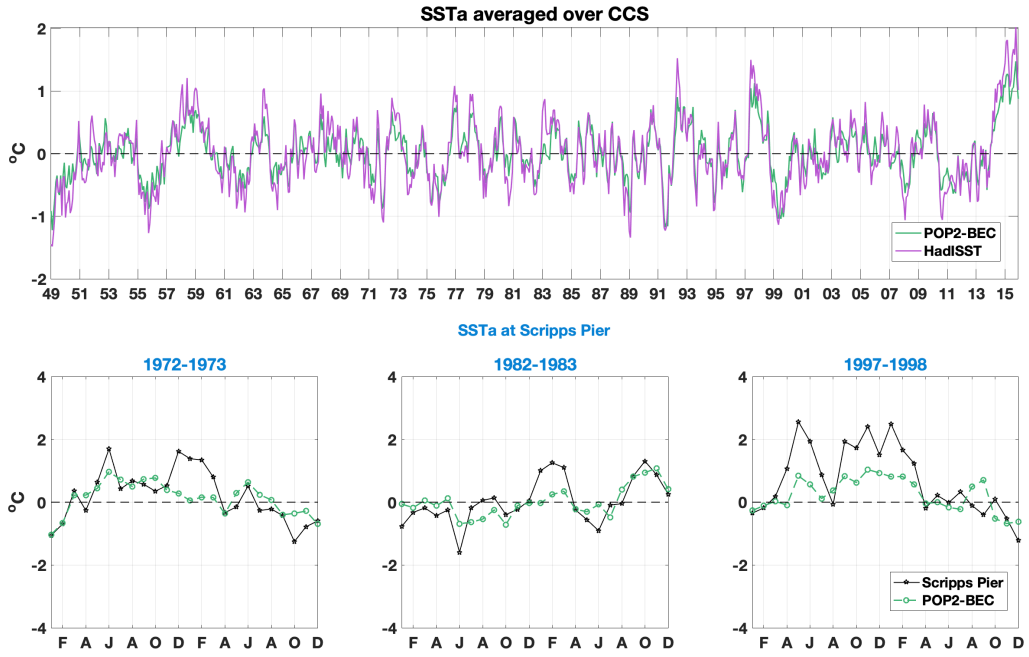

Figure 2.3 a) Modeled SSTa (blue) averaged over the CCS region (21-48 °N) along with the observed averaged anomalies from HadISST (orange). Correlation between the time series is 0.93 and RMS is 0.5 °C and 0.24 °C respectively. b), c), d) SSTa over a single point over Scripps Pier at La Jolla CA. Model (black dashed line) and from observations (blue solid line) for three specific El Niño events as indicated by the years at the top.

2.3.2 Lagged correlations of the CCS with ENSO

In order to obtain a broad-brush view of the CCS response to ENSO in the CESM-POP2-BEC simulation, we computed the correlation of the ONI in the tropical Pacific with the physical-biological fields in the CCS at various lags (zero to 9 months). Rather than showing all the lagged-correlation results, Fig. 2.4 shows only the model's 3-month lagged-correlation

response between observed ONI and the POP2-BEC fields (including all months) for SSTa, pycnocline depth and biogeochemistry over the CCS. The 3-month lag was chosen because it is able to simultaneously capture key aspects of both the well-developed physical response (after the winter peak of the atmospheric teleconnection forcing) and the still developing biological response in early spring. The results reveal the anticipated basic structure of warming, thermocline deepening, and decreased nutrient and plankton concentrations along the coast during El Niño events (*e.g.,* Schwing *et al.,* 2005). As expected from previous studies (*e.g.,* Alexander *et al.,* 2002; Turi *et al.,* 2018), the maximum correlations of the ONI with the CCS response tend to occur at lags of several months. SSTa exhibits greatest lagged correlations over southern Baja California and Oregon, and weaker ones along the California coast, consistent with the coherency shown by EOF1 of the model SST. The pycnocline depth correlations are more confined to the coastal regions than those for SST, which extend further offshore.

Correlations of the biogeochemistry (average nitrate concentration from 25m-100m and oxygen at 200-m depth) are closely related to those shown by the anomalies of the pycnocline depth. Correlations of 0m-100m vertically averaged chlorophyll and zooplankton are highest over southern Baja California but still significant up to the central California region. The chlorophyll and zooplankton responses (shown in detail below) expand northward and increase in magnitude later in spring and summer but fail to cover the coast of northern California and Oregon where significant ENSO-coherent anomalies are typically observed (*e.g.,* Thomas *et al.,* 2009, 2012). The reasons for this discrepancy are not obvious but may be due to a combination of the errors in the physical circulation as well as to the oversimplified ecosystem formulation.

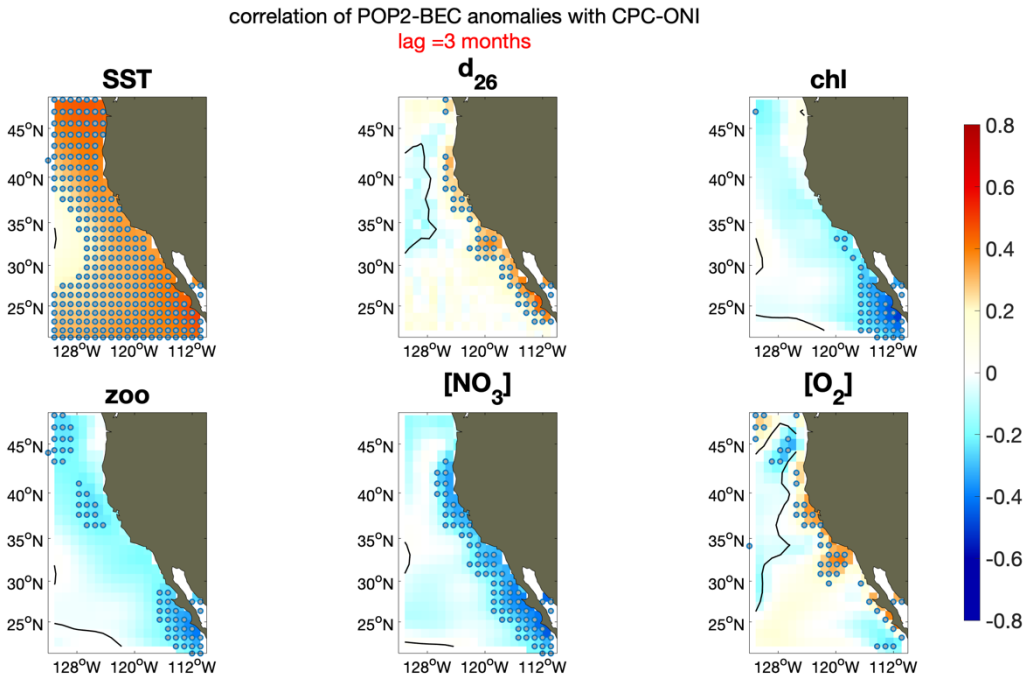

Figure 2.4 Lagged (3-month) correlations of tropical Pacific ONI with anomalies of SST, pycnocline depth, vertically averaged chlorophyll, zooplankton biomass, average [NO_3] over 200m, and [O_2] at 200m.

2.3.3 A composite physical-biological ENSO in the CCS

We next examine the response of the whole CCS during ENSO events, using spatially explicit composite anomalies of SST, pycnocline depth, 0m-100m vertically averaged chlorophyll, 0m-100m vertically averaged zooplankton biomass, 25m-100m vertically averaged nitrate, and oxygen at 200m depth. Typically, warm (cold) anomalies related to El Niño (La Niña) peak during the winter (DJF) after developing during the previous fall (SON). For sake of simplicity, we show only the months in which the ENSO-related SST anomalies are typically the largest. Each of the field-map composite anomalies of SST shows September through December of the pre-peak year, and January through April of the following year corresponding to the peak and post-peak of the event. The pycnocline, chlorophyll, zooplankton biomass, [NO_3], and

dissolved [O_2] composite anomalies are shown for January through August of the post-peak year because biological variables exhibit their largest ENSO-related signals after the spring bloom.

2.3.3.1 SST and pycnocline depth anomalies

The SSTa over the CCS (Fig. 2.5) show the evolution of the model composite El Niño during its development in the fall and maturation in the winter. The surface of the ocean starts warming during the fall (SON) of the year previous to the peak of the event (top panel) but anomalies do not become statistically significant until they reach maximum (warmer) values during FMA of the post-peak year. Only in these months is the warming related to El Niño significant in the northern California Current region. In the Southern California Bight significance levels are only above 1 standard deviation from the bootstrap analysis (above 67% but below 95%, not shown). As expected from the EOF and correlation analyses, warming also occurs along Baja California, although it does not reach our level of significance. The cool SST that develops far offshore is the eastern extent of the cold central Pacific SST that develops during El Niño due to the strengthened Aleutian Low, and is associated with the spatial pattern of the Pacific Decadal Oscillation (*e.g.,* Newman *et al.,* 2016).

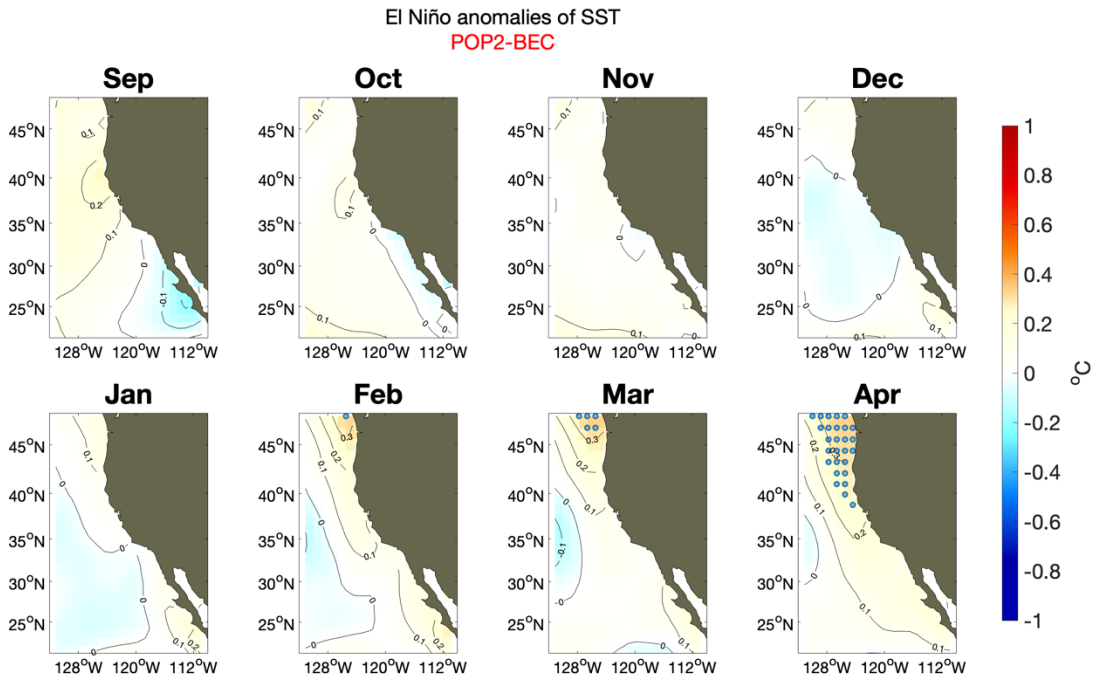

Figure 2.5 Composite El Niño SSTa. Significant warm (red) anomalies above the 95% confidence level are marked in black circles.

The evolution of the model composite SSTa during La Niña (Fig. 2.6) shows the beginning of the cold phase in late fall of the pre-peak year (top panel) with intense cold anomalies off Baja California Sur. Negative anomalies exhibit the coldest temperatures during JFM, as shown in the lower panel of Fig. 2.6 (post-peak year). Note how the SST anomalies related to La Niña are significant (above 2 standard deviations) over broad regions offshore and along the coast in most of the region, even during the fall preceding the peak of the cold event. In contrast to the El Niño model composite, La Niña develops earlier, more strongly, and over broader areas than El Niño, indicating that the response of the CCS is asymmetric (*e.g.,* Fiedler and Mantua, 2017). This asymmetry will be more extensively explored in later sections.

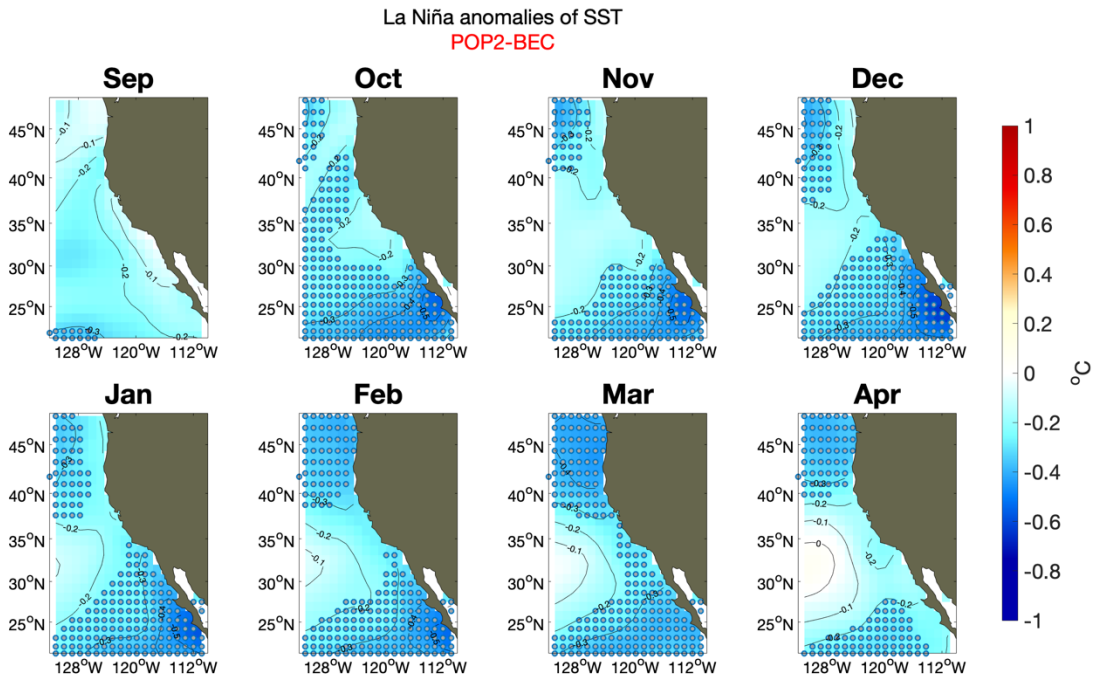

Figure 2.6 Composite La Niña SSTa. Significantly cold (blue) anomalies above the 95% confidence level are marked in black circles.

The composite evolution of observed SSTa during El Niño and La Niña events is shown in Fig. 2.7 and Fig. 2.8, respectively. Composite anomalies from the HadISST record generally show similar spatial patterns to those in the model for both warm and cold events. The magnitudes (and consequent significance) of the anomalies are generally much higher in the observations, however, especially along the coast of Baja California during the peak of warm events in DJF. We note that the observed composite anomalies also reveal more intense (and more significant) anomalies during La Niña events compared to El Niño, with the winter after the La Niña peak exhibiting a significant cooling of the whole CCS (Fig. 2.8). This asymmetry is consistent with what was found for the model composite in Figs. 2.5 and 2.6.

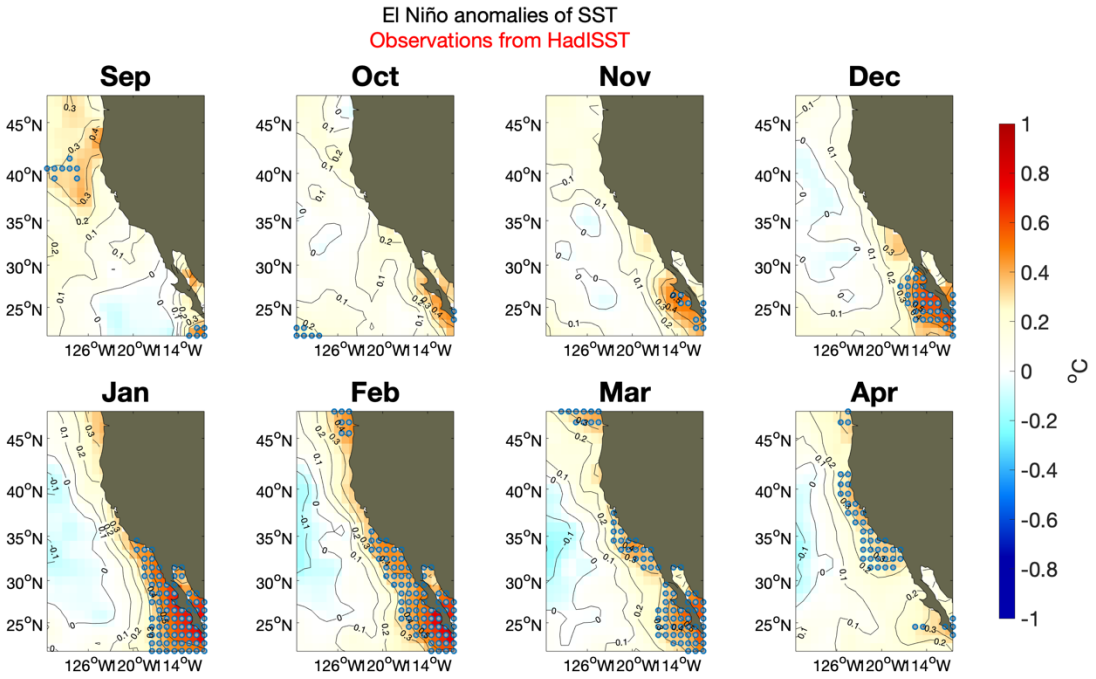

Figure 2.7 Observed (HadISST) composite SSTa from 13 El Niño events in the period from 1949-2015. Significant warm (red) anomalies above the 95% confidence level are marked in black circles.

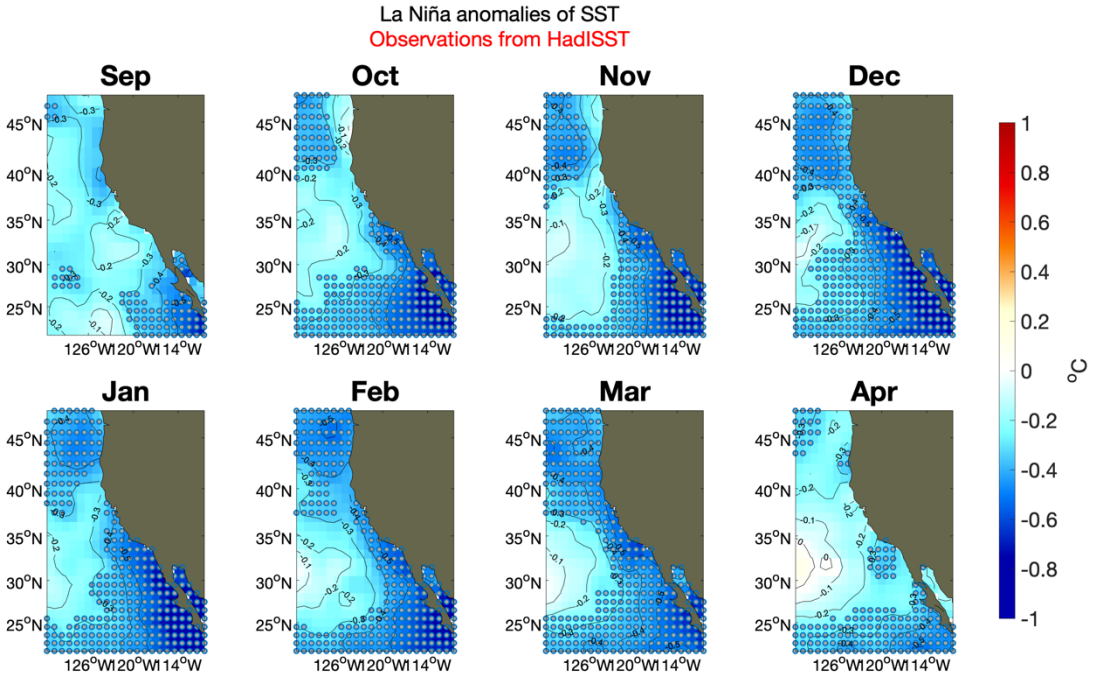

Figure 2.8 Observed (HadISST) composite SSTa from 13 La Niña events in the period from 1949-2015. Significantly cold (blue) anomalies above the 95% confidence level are marked in black circles.

The pycnocline depth composite over the CCS was calculated using the σ=26 isopycnal surface as a proxy (*e.g.,* Di Lorenzo *et al.,* 2005; Kim and Miller, 2007). It is typically located between 180m and 250m in the model, while in nature the depth is often shallower, roughly 50m to 200m depths (*e.g.,* Rudnick *et al.,* 2017). As anticipated from the correlation analysis, the composite El Niño anomalies for the post-peak year (Fig. 2.9) show a deepening of the pycnocline that starts developing during January and February along the coast, peaks during the spring, and persists into the summer season. During La Niña (Fig. 2.10), the reverse occurs in the composite, as a significantly shallower thermocline starts developing off the coast of Baja California during February, and the anomalies intensify during the spring and the summer. The CCS pycnocline depth response to ENSO is mainly confined to the coastal region, and at early stages is only significant at southern latitudes in the regions adjacent to the coast. This is consistent with what is observed in other studies that also report a latitudinal dependence in the response of the pycnocline (Jacox *et al.,* 2015; Frischknecht *et al.,* 2015), as well as in other variables such as sea-surface height and average temperature of the upper 100 m (Crawford, 2017).

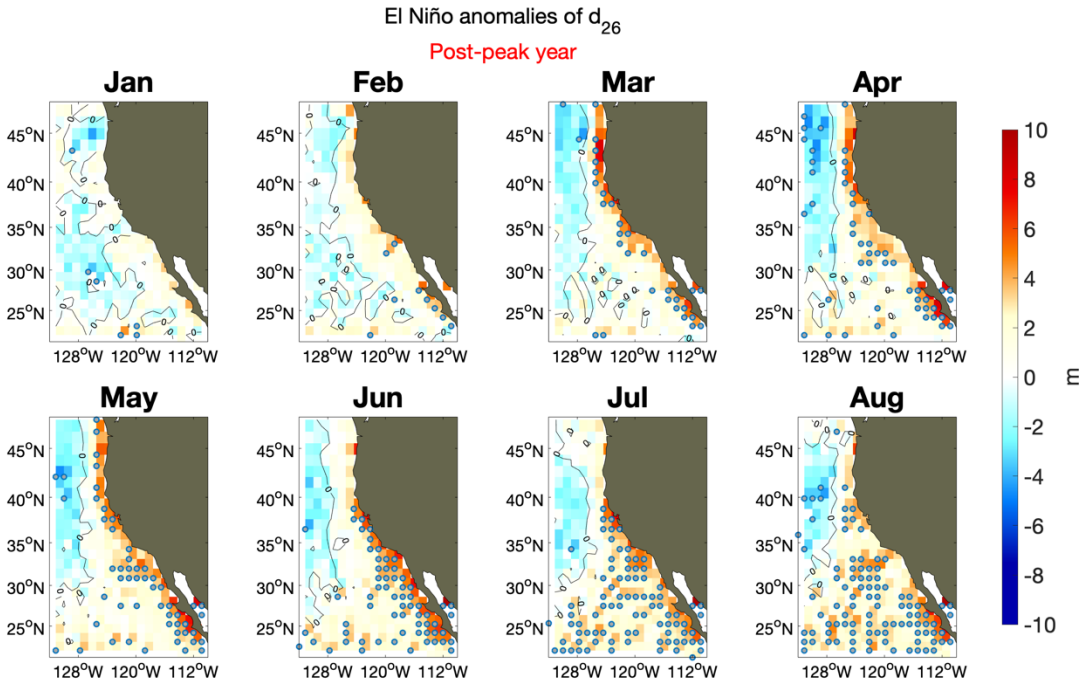

Figure 2.9 Modeled composite El Niño pycnocline depth anomalies, (d26). Significantly deep (red) anomalies above the 95% confidence level are marked by gray circles.

A deeper pycnocline is expected over the CCS during El Niño due to the southerly wind anomalies acting to suppress upwelling as well as from remotely driven coastally trapped Kelvin-like waves (Chávez and Messié, 2009; Jacox *et al.,* 2015; Frischknecht *et al.,* 2015). However, the coarse resolution model cannot properly resolve this Kelvin-like wave propagation effect, so that even though the model exhibits deeper (shallower) values associated with El Niño (La Niña), the response can be muted with respect to the observed variability (*e.g.,* Hsieh *et al.,* 1983). Comparing our results to the data assimilated ocean analysis study of Jacox *et al.* (2015) indicates that the ENSO-forced pycnocline response in CESM-POP2 is lagged by 1-to-2 months depending on the latitude along the California Coast. The anomalies of the pycnocline depth reach their peak during the spring (March-April) in the southern CCS, and after this season over northern locations. Jacox *et al.* (2015) also report that the timing of the ENSO-forced minimum

depth of the pycnocline depends on latitude, but that it varies from March-April off central California to June-July off the Oregon coast. The mismatch with the data-assimilated product is likely due to the coarse resolution, which cannot resolve the upwelling that occurs on the Rossby deformation-radius scale that ranges from ~20km in the northern CCS coast to ~40km along the southern Baja California coast (*e.g.,* Chelton *et al.,* 1998). These local coastal effects thereby become diluted into broader areas adjacent to the coast where other large-scale processes of surface-heating, advection, and open-ocean upwelling can interact with that coastally driven response.

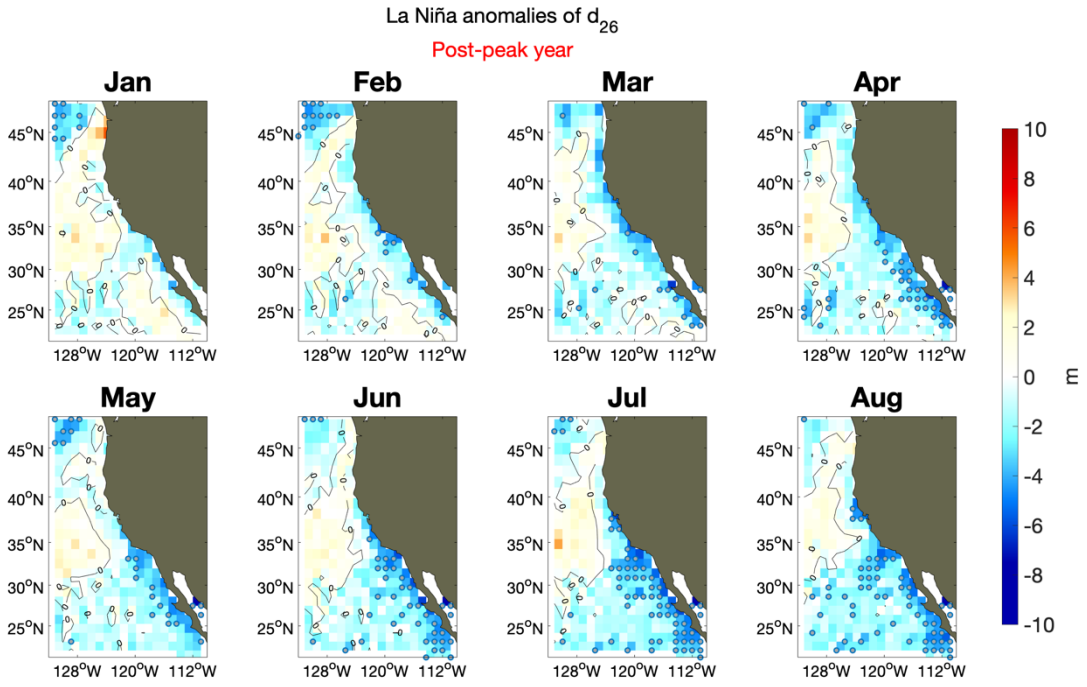

Figure 2.10 Modeled composite La Niña pycnocline depth anomalies, (d26). Significantly shallower (blue) anomalies above the 95% confidence level are marked by gray circles.

2.3.3.2 Chlorophyll

Turning our attention to a biological variable, Fig. 2.11 shows the composite anomalies of the 0m-100m vertically averaged chlorophyll (including all 3 phytoplankton groups) from January to August of the post-peak year of El Niño. The structures seen in chlorophyll are less organized than for the physical variables. As anticipated from the 3-month lagged-correlation with the tropical Pacific ONI (Fig. 2.4), negative chlorophyll anomalies (with small amplitudes of ~1-3% of the typical seasonal mean values) along the Baja California coast are the most consistent feature throughout the post-peak composite. They turn significantly negative during April off both Baja and central CCS, and then persist into the summer, extending further north through July and August. This response is coherent with the timing of the anomalies of the model pycnocline depth, and with its latitudinal dependence. While pycnocline anomalies show a delay with what is typically observed, chlorophyll anomalies occur within the time frame observed by previous studies (*e.g.,* Thomas *et al.,* 2012; Kilpatrick *et al.,* 2018). Anomalous patches of relatively high chlorophyll are shown at the Oregon coast and off-shore during January through March, but they are not significant and are likely due to errors in the interpolation of the wind forcing near the coastal boundary or errors in the model.

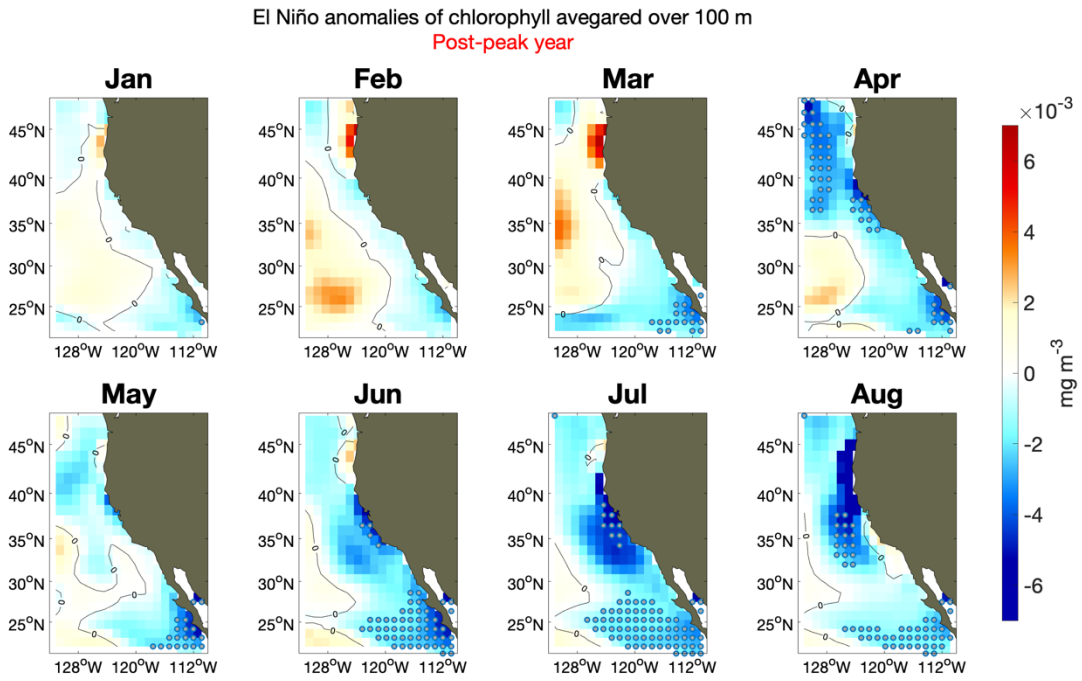

Figure 2.11 Modeled post-peak El Niño composite vertically averaged (down to 100 m) chlorophyll anomalies. Significantly lower chlorophyll anomalies (blue) are marked by gray circles.

Fig. 2.12 shows the analogous evolution of the composite chlorophyll anomalies during La Niña. Late spring (April-May) and summer months during the post-peak year of the composite are dominated by the positive anomalies of chlorophyll (~1-3% of typical seasonal mean values), showing that the model captures the enhancement of the climatological spring bloom (McGowan *et al.,* 2003; Kim *et al.,* 2009; Thomas *et al.,* 2012; Goebel *et al.,* 2010). The composite response of the CCS chlorophyll during La Niña is also coherent with the variability of the pycnocline depth and offshore SSTa, and also shows a latitudinal differentiation. Negative chlorophyll anomalies prevail off the Oregon and Washington coasts throughout this post-peak period, a result that is opposite to what observed, although not significant (*e.g.,* Fig. 7a of Thomas *et al.,* 2012), indicating potential errors in the model or forcing fields.

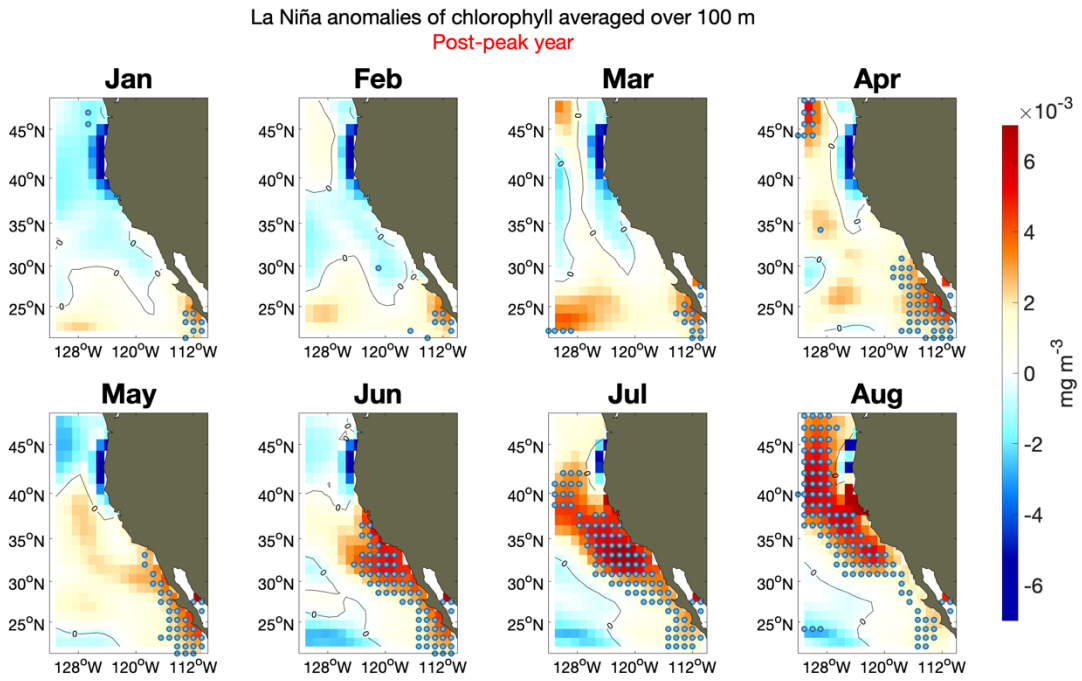

Figure 2.12 Modeled post-peak La Niña composite vertically averaged (surface to 100 m). Significantly higher chlorophyll anomalies (red) are marked by gray circles.

Since chlorophyll is computed in the model as a nonlinear relationship involving the three phytoplankton components and other variables (*e.g.,* Moore *et al.,* 2002), we computed composites of the biomass of diatoms, diazotrophs, and small phytoplankton separately to determine if any of them behaved more coherently in their response to ENSO variations. Both the diatoms and the small phytoplankton exhibited the same basic features seen in the chlorophyll composites. The diazotrophs, in contrast, had very small biomass compared to the other two phytoplankton and were limited spatially to offshore regions in the southern CCS domain. Therefore, the chlorophyll composites give an accurate depiction of the model's ability to represent the large-scale coherent phytoplankton biomass response to ENSO-related variations.

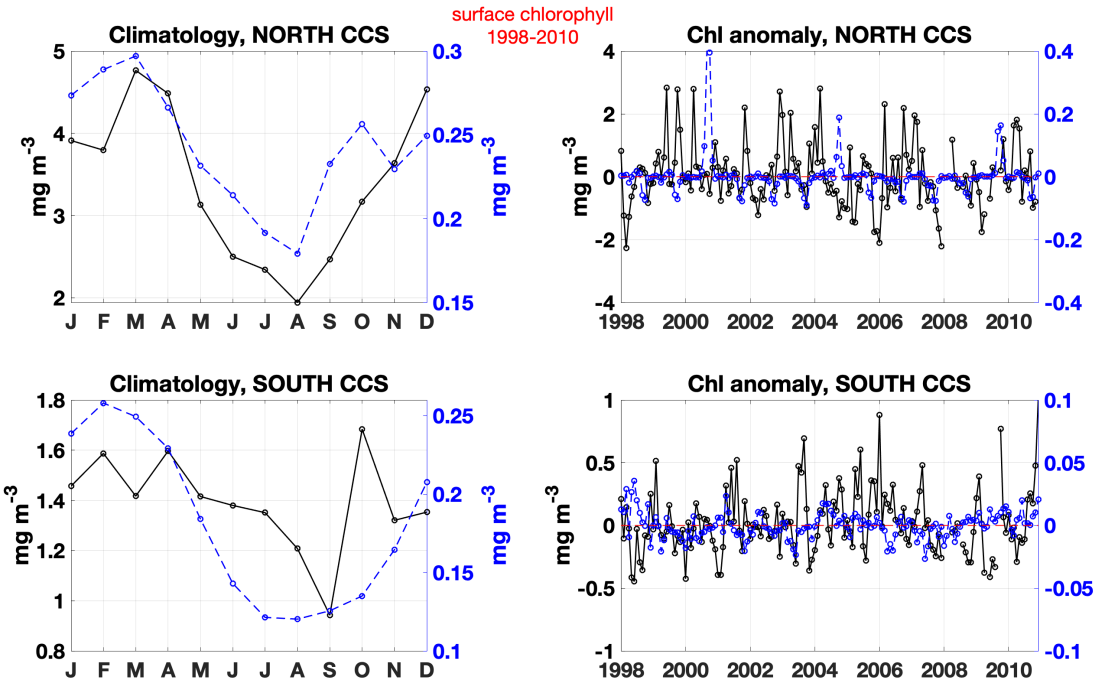

Figure 2.13 Comparison of (vertically averaged, surfaceto 25 m) chlorophyll from BEC (blue) with SeaWiFS (black) for North CCS (38-47 °N) and South CCS (32-38 °N). Climatological values are shown in the left panels and the right panels represent the anomaly time series for the period 1998-2010.

To further explore the model's ability to represent chlorophyll compared to nature, the CCS was divided into two sub-regions and compared to surface chlorophyll of satellite observations from SeaWiFS. Two boxes were selected: southern CCS is located between 32-38 °N and northern CCS between 38-47 °N, both with an approximate extension of 400 km from the coast. The model was averaged down to a depth of 25 m for comparison with the observations that sample an optical depth. Climatological values of chlorophyll from the period of 1998-2010 are shown in the left panels of Fig. 2.13. The model severely underestimates the mean values as indicated by the different y-axes scales. This is consistent with the analysis of Moore *et al.,* (2004, their Fig. 3) who showed very weak mean springtime chlorophyll in the CCS region for BEC compared to other areas where the model compared better with satellite observations. Both

the climatological values and the anomalies are one order of magnitude smaller than in observations. The seasonal timing of the modeled mean chlorophyll is generally consistent with the observations in the northern part of CCS. Both peak during wintertime (DJF) and early spring (MA), and consistently decrease during summertime (JJA). The modeled variability in the southern CCS shows some differences compared to the observed timing, particularly during the summer months (JJA) where the modeled values drop down but the observed chlorophyll persists from winter through August. Surface chlorophyll anomalies from the model in the CCS are in poor agreement with the satellite surface observations over the 1998-2010 time period as indicated by the small and insignificant correlations in both the north and south CCS regions when including all months (i.e., for El Niño, La Niña, and neutral conditions together). This is in contrast to the composites that reveal coherent signals (although very small) associated with the warm and cold ENSO events.

2.3.3.3 Nutrients and dissolved oxygen

The model composite evolution of [NO_3] anomalies during El Niño is shown in Fig. 2.14. In contrast with the chlorophyll response that shows marked differences with latitude, nitrate concentrations seem to respond uniformly along the CCS during the spring, when negative anomalies associated with El Niño reach their maximum in the model. This variability is very coherent with the timing shown by the anomalies of the pycnocline depth, as would be expected from the results of the correlation analysis. Depleted nutrient concentrations during El Niño are consistent with the typically downwelling-favorable anomalous wind fields (*e.g.,* Jacox *et al.,* 2017), consequent deepening of the pycnocline, and muted upwelling of source waters. The opposite situation occurs during La Niña (Fig. 2.15), when intensified upwelling favors higher

[NO_3] that starts to show as early as February in the southern CCS and peaks during the spring over the whole CCS. Both El Niño and La Niña composites show anomalies that persist through the summer, consistent with chlorophyll anomalies. The magnitude of these nitrate anomalies, ~0.5 mmol m^{-3}, is rather small compared to typical mean values of 20 mmol m^{-3}. But this is to be expected for monthly mean anomalies because of the rapid response time (~days) of phytoplankton in the euphotic zone that results in an equilibrated balance between vertical nutrient flux, uptake by phytoplankton, and grazing by zooplankton.

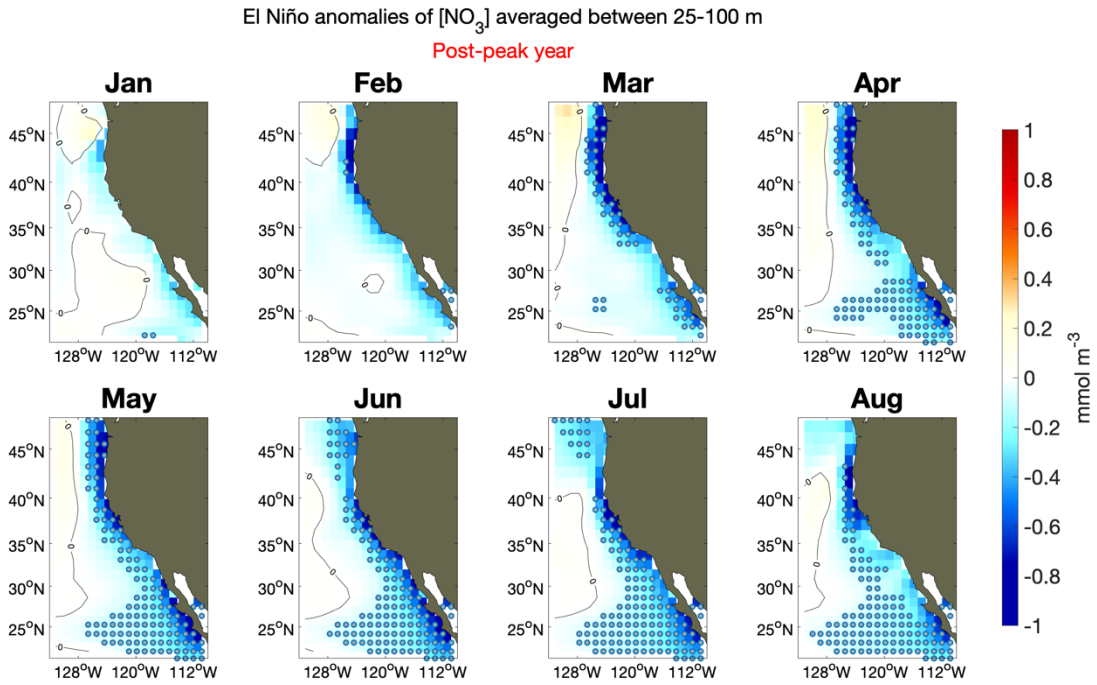

Figure 2.14 Modeled post-peak El Niño composite of [NO_3] averaged between 25m to 100 m. Significantly lower anomalies (blue) are marked by gray circles.

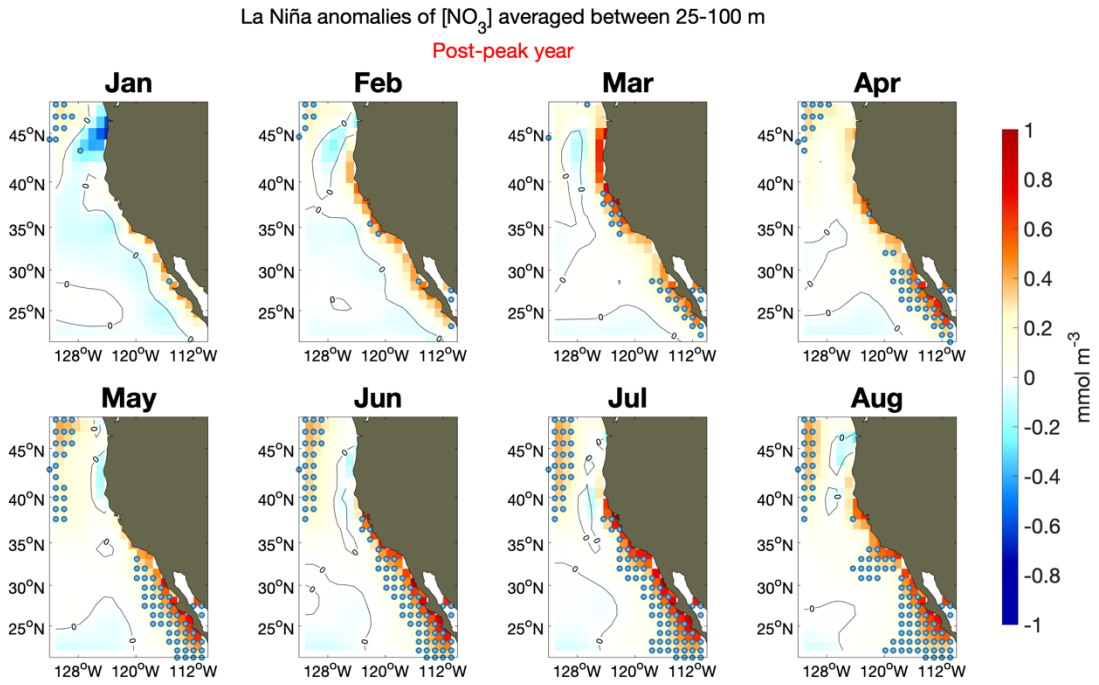

Figure 2.15 Modeled post-peak La Niña composite of [NO_3] averaged between 25m to 100 m. Significantly higher anomalies (red) are marked by gray circles.

Composite dissolved oxygen concentrations at 200m show patterns similar to the nutrient composites. During El Niño events the pycnocline is depressed, which then acts to push down the oxygen minimum zone in the areas adjacent to the coast, resulting in relatively higher dissolved [O_2] at 200m (Fig. 2.16). The opposite situation occurs during La Niña events (Fig. 2.17), when upwelling of isopycnal surfaces shifts the level of minimum oxygen to shallower depths, and dissolved [O_2] is depleted ~3-5 mmol m^{-3} relative to normal conditions (~50 mmol m^{-3}) at 200 m. (The model composites also reveal oxygen anomalies of reversed sign off the coast of Washington, although they tend to lack statistical significance.) Our results are consistent with those shown by Turi *et al.,* (2018), where their composites of oxygen at 100 m reveal an increase in dissolved [O_2] during warm events. The response shown by their results is

also confined to a coastal band that extends ~200 km offshore, while most of the deeper ocean shows little response to El Niño.

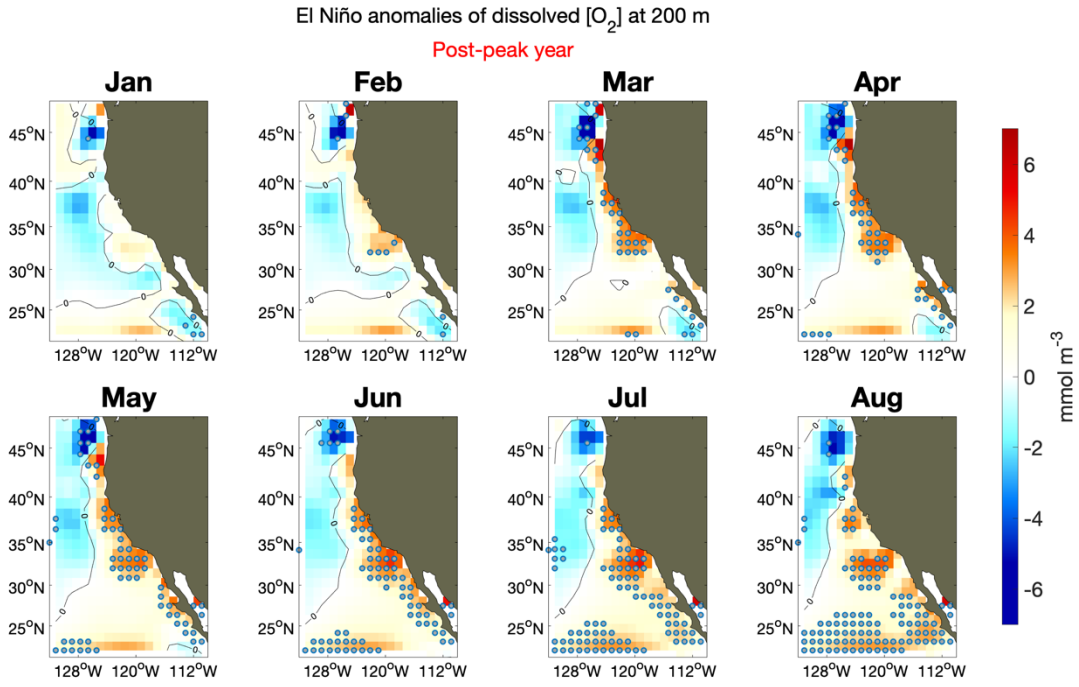

Figure 2.16 Modeled post-peak El Niño composite [O_2] at 200m depth. Significantly higher values (red) are marked by gray circles.

We emphasize that the composite variability of dissolved oxygen and nutrients represented by the model is limited by the coarse resolution to include only large-scale processes and parameterized eddy-mixing effects. This results in a relatively simple link between the large-scale changes imprinted by the ENSO and the direct effects on nutrients and [O_2] that are mainly determined by changes in the thermocline depth. Unresolved mesoscale and submesoscale processes that contribute to lateral and vertical mixing can also play a different and very important role in altering these patterns (*e.g.,* Gruber *et al.,* 2011; Di Lorenzo *et al.,* 2013; Jacox *et al.,* 2015; Frischknecht *et al.,* 2018), which should be explored in additional work.

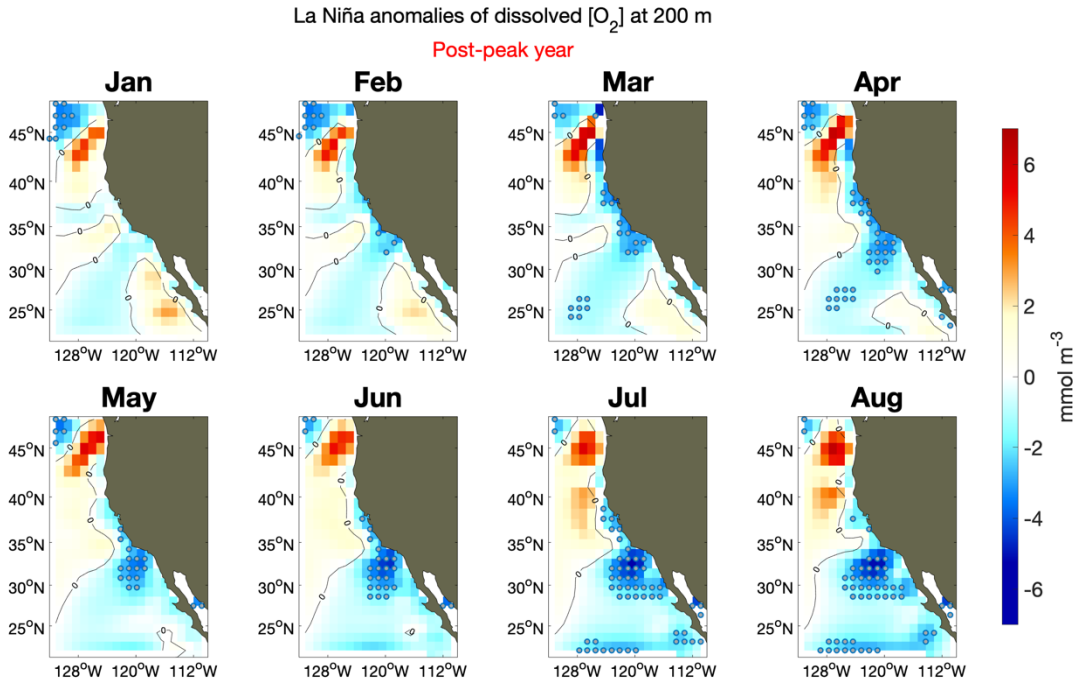

Figure 2.17 Modeled post-peak La Niña composite [O_2] at 200m depth. Significantly lower values (blue) are marked by gray circles.

2.3.3.4 Zooplankton

Fig. 2.18 represents the composite evolution of the post-peak year of El Niño for the zooplankton group in the model. The response resembles the one shown by the chlorophyll anomalies (see Fig. 2.11), with negative values that are well developed by summer (JJA), but are weaker in winter and early spring. The modeled zooplankton also exhibits a stronger (and more significant) response during La Niña (Fig. 2.19) compared to the composite El Niño, and positive blooms begin off the coast of Baja California during Jan-Feb, persisting through the spring and extending further north in the CCS in the summer. The magnitude of the zooplankton anomalies coherent with ENSO in the model is a few percent of the mean background state.

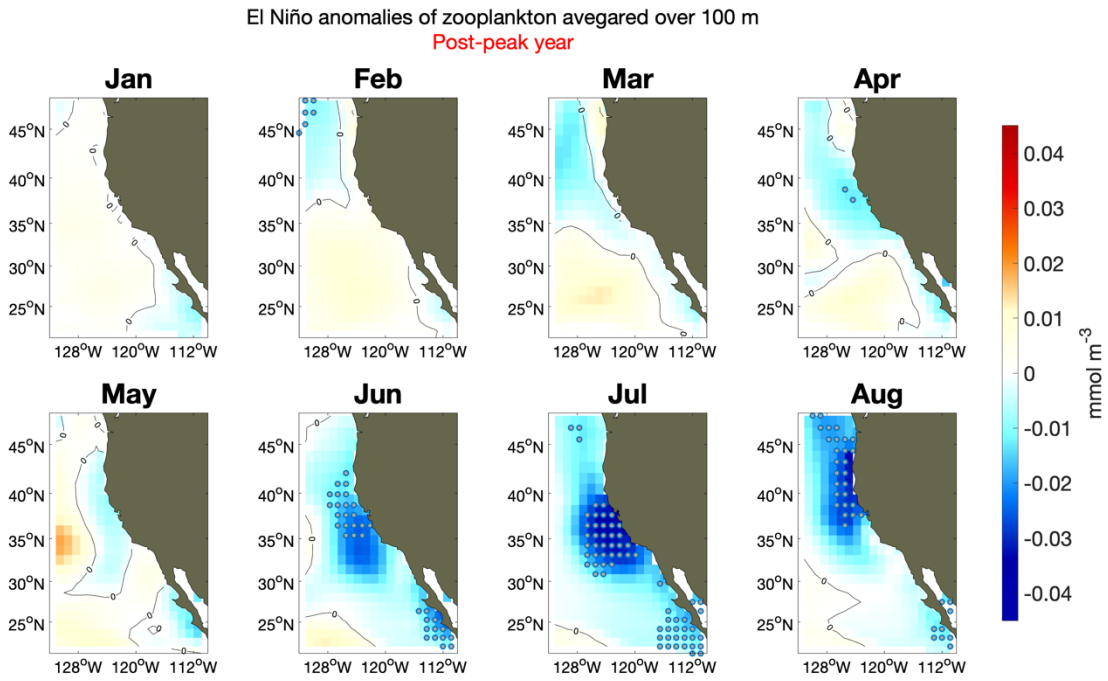

Figure 2.18 Modeled post-peak El Niño composite vertically averaged (surface to 100 m) zooplankton biomass anomalies. Significantly lower anomalies (blue) are marked by gray circles.

While some previous studies have shown a rather direct link between ENSO conditions and zooplankton (*e.g.,* Bograd and Lynn, 2001; Fisher *et al.,* 2015), one recent study on samples from CalCOFI cruises suggests that changes in zooplankton community can only be related to El Niño at the level of species and individual taxonomic groups. Although some taxa, such as euphausiids and calanoid copepods, showed a decline in biomass during El Niños 1958, 1959, 1983, 1992, 1993, 1998, 2003, 2010, and 2016, total mesozooplankton biomass does not vary consistently (Lilly and Ohman, 2018). The same study reports that some of the species of copepods and euphausiids actually decreased in biomass during la Niña (for years 1951, 1956, 1965, 1989, 1999, 2000, and 2008).

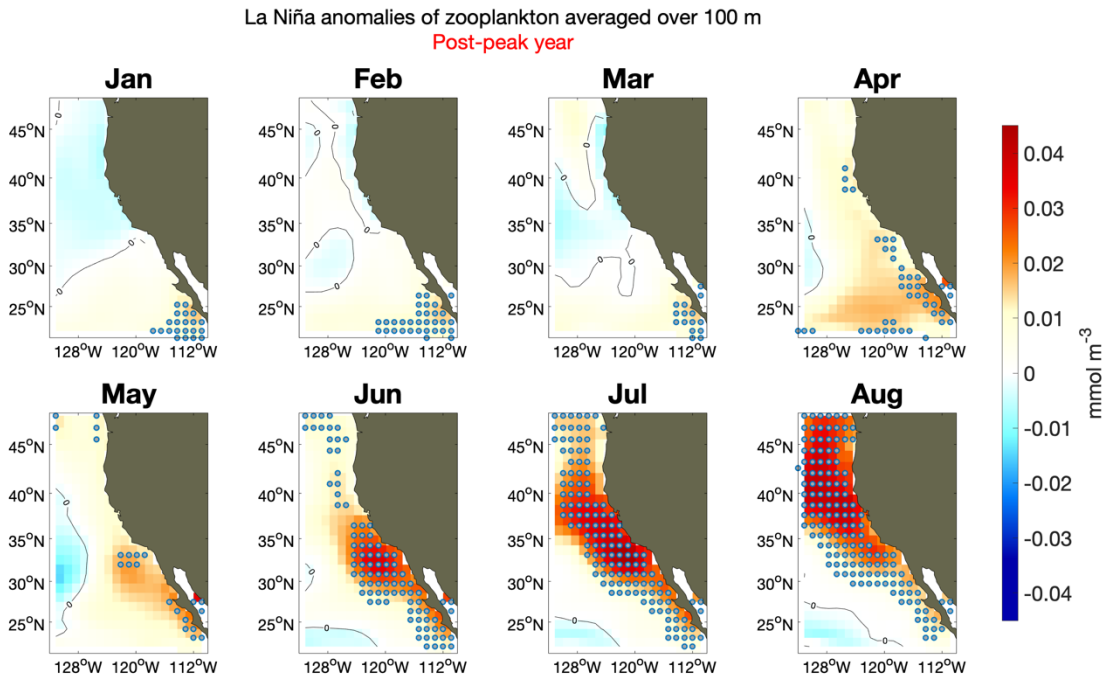

Figure 2.19 Modeled post-peak La Niña composite vertically averaged (surface to 100 m) zooplankton biomass anomalies. Significantly higher anomalies (red) are marked by gray circles.

The zooplankton included in the model is a simplified formulation as an aggregate group that includes microzooplankton and mesozooplankton with no representation of a particular group. The response of the CCS shown by the composite anomalies seems to be very well defined as negative values during El Niño and positive during La Niña, with a strong correlation to model phytoplankton, while observations indicate that zooplankton community is not consistently affected during warm versus cold ENSO events.

2.4 Discussion

A physical-biological ocean model hindcast of the time period 1949-2015 was analyzed to establish its skill levels on interannual timescales when compared with available observations and to construct composite El Niño and La Niña events for the California Current System. We

found that when averaging the model response over the entire CCS, it well reproduces the SSTa estimated from HadISST. When considering smaller regional averages or individual points (such as Scripps Pier), the model exhibits less coherency with SST observations and tends to have a lower amplitude. Much of this disagreement can be ascribed to the coarse resolution (~1°) of the simulation, but issues associated with errors in the surface forcing functions may also be involved. For example, the interpolation scheme for the winds incorporates winds over land for oceanic grid points adjacent to the coast, which can adversely affect the coastal upwelling and offshore wind-stress curl fields that provide the dominant forcing of the coastal ocean.

There are many approaches to identify the effects of ENSO over the CCS. For instance, one could treat each ENSO event individually as has been done previously in many case studies (*e.g.,* Bograd and Lynn, 2001; Frischknecht *et al.,* 2017), which corresponds to the extreme view that each ENSO event is totally different from other events due to differing tropical teleconnections or to random variability of the midlatitude weather systems (e.g., Deser *et al*., 2018; Capotondi *et al*., 2019). But the composite approach is useful to provide a picture of the consistent types of responses that would be expected to be found for a typical event. One could alternatively also separate the warm and cold events into finer-grained samples, *e.g.,* associated with Central Pacific vs. Eastern Pacific events (*e.g.,* Ashok *et al.,* 2007; Di Lorenzo *et al.,* 2010; Capotondi *et al.,* 2019), or perhaps using some other criterion to create even more groups of warmish or coldish events. However, as Capotondi *et al*. (2015) clearly state, there is no strict bimodality evident in the ENSO distribution, which may be more properly defined as a continuum. Among the many different ways to address the topic, we chose a composite approach

using 14 warm and 15 cold, moderate-to-large events to give a general view of the CCS response in the CESM-POP2-BEC simulation.

The maps of model ENSO composite anomalies exhibit their strongest signals in the post-peak winter and spring for SST and pycnocline depth, and in the post-peak winter through summer for chlorophyll, zooplankton biomass, [NO_3], and dissolved [O_2]. While SST responds relatively uniformly over the whole north-south region of the CCS during model ENSO events, the response of the pycnocline depth and the biogeochemistry shows a latitudinal dependence that was also noted in previous studies using observations and models (Chenillat *et al.,* 2012; Jacox *et al.,* 2015; Crawford *et al.,* 2017). Oxygen at 200m is controlled in the model mainly by the physical forcing associated with changes in upwelling and downwelling, but we did not explore potential influences of horizontal ocean currents or changes in oxygen solubility.

The response of the ENSO composite pycnocline depth in the model is delayed by a period of 1 to 2 months compared to observations (*e.g.,* Lynn and Simpson, 1987; Collins *et al.,* 2003; Jacox *et al.,* 2015). More recently, Crawford (2017) used a multivariate EOF analysis of an ocean data assimilation product to show that peak anomalies of the pycnocline depth occur during February over the CCS, which is 1-to-2 months earlier than we found here. While further study is necessary to explain this delayed isopycnal response in POP2-BEC, we can speculate about some of the possible mechanisms that may lead to this delay. The ocean component of the model is forced by observed winds from reanalysis, clearly accounting for the local changes in the pycnocline depth induced by the variability of the local wind stress along the California Coast. Yet the model coarse resolution will suppress (*e.g.,* Hsieh *et al.,* 1983) the remotely

forced variability of coastal-trapped Kelvin-like waves propagating northward along the coast that affect the pycnocline (*e.g.,* Frischknecht *et al.,* 2015). Additionally, the coarse resolution spreads the impact of nearshore wind stress over a broader area, thereby reducing the strength of both coastal upwelling and wind-stress-curl forced upwelling along an eastern boundary (Song *et al.,* 2011; Small *et al.,* 2015). These various effects may contribute to the delay in upwelling timing but additional work is required to identify the processes that can be improved in the model and should be addressed in future research.

The composite results for the model biological and chemical variables are dependent on the quality of the physical drivers. Even with the noted deficiencies of the physical state during ENSO events, coherent signatures of the ecology and biogeochemistry appear in the model composites. These variables tend to exhibit their most significant response in conjunction with the model's most consistent pycnocline response, which tends to be post-peak winter through summer for the ENSO events. This important link between the pycnocline and the modeled ecological response should be further explored in future modeling studies that include much higher resolution in the regional ocean (Curchitser *et al.,* 2013; Frischknecht *et al.,* 2015, 2017; Jacox *et al.,* 2015).

The model composite CCS anomalies during El Niño and La Niña events reveal an asymmetry in that a stronger and more statistically significant La Niña influence on SSTa occurs compared to the El Niño influence, as previously discussed by Fiedler and Mantua (2017) for observations. This asymmetry also occurs prominently in the vertically averaged chlorophyll and zooplankton composite anomalies, but is less evident in the isopycnal, nitrate and oxygen fields.

This cold-event asymmetry in the CCS is somewhat unexpected, since typically El Niño events exhibit a stronger SSTa in the eastern tropical Pacific than La Niña (Rodgers et al. 2004; An and Jin, 2004; Levine *et al.,* 2016; Burgers and Stephenson, 1999), an aspect related to ENSO nonlinearities (Rodgers *et al.,* 2004). To further explore this asymmetry, Fig. 2.20 shows the histograms of modeled (left) and observed (right) monthly-mean SSTa averaged along the coastal region of the CCS for months corresponding to neutral (top), El Niño (middle), and La Niña (bottom) events. The distributions reveal the tendency of the model to produce weaker variability than observations, for both neutral years and ENSO events. For both model and observations, the SSTa events in the CCS that are associated with La Niña cluster more consistently around negative values (as also discussed by Fiedler and Mantua, 2017, and seen in Fig. 5g of Turi *et al.,* 2018), indicating the mean of the distribution shifting below zero. In contrast, both modelled and observed CCS SSTa associated with El Niño events, although they include the most extreme warming conditions (*e.g.,* McGowan *et al.,* 1998), are often cool or only very weakly warm, and are more symmetrically distributed around zero anomaly. This results in a mean model El Niño composite response that is weaker, and less significant, than for model La Niña events. Our observed composites from the HadISST also reveal that the asymmetric response favoring La Niña is not an artifact of the model. This asymmetry is also clearly evident in the ordination diagram of Fielder and Mantua (2017) and the mean composite warm and cold events plotted in Fig. 5g of Turi et al. (2018).

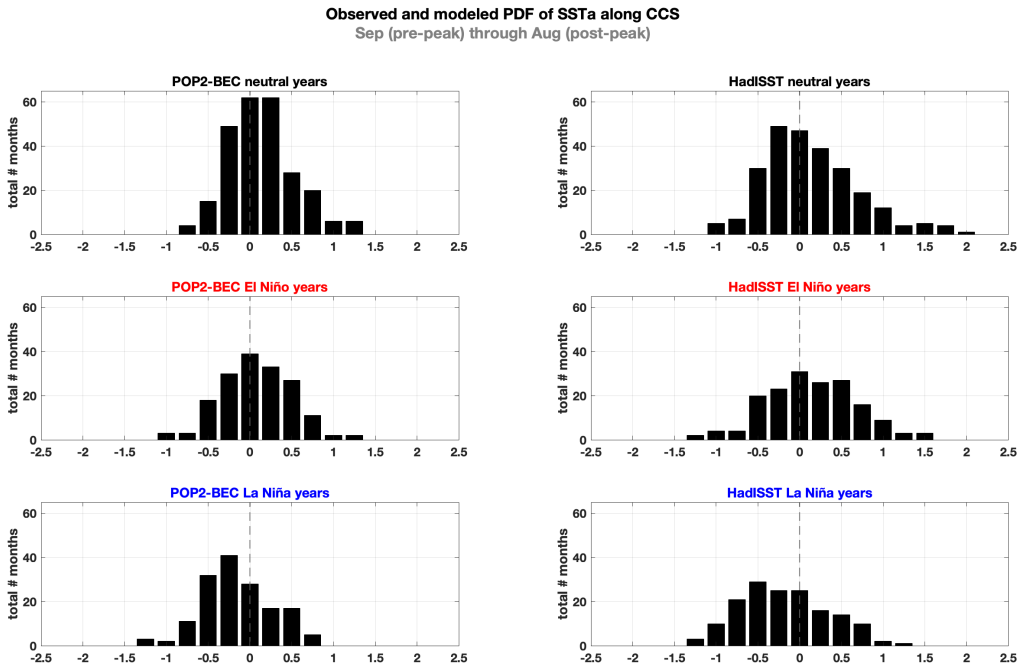

Figure 2.20 Histograms of modeled (left) and observed (right) SSTa for pre-peak September through post-peak August over CCS for neutral, El Niño, and La Niña years. Model neutral years have a mean (μ) of 0.13 and a STD (σ) of 0.40, while observed neutral years have μ=0.14 and σ=0.57. Model warm events (μ=0.08, σ=0.41), have 57% of their months positive, while model cold events (μ=-0.15, σ=0.41) have 68% of their months negative. Observed warm events (μ=0.15, σ=0.55) have 60% of their months positive, while observed cold events (μ=-0.18, σ=0.53) have 65% of their months negative.

To further study the mechanism behind this asymmetric response, we examined whether the asymmetry arises in the tropical Pacific or is locally generated by the CCS winds. Fig. 2.21 (top) shows histograms of the observed SST anomalies in the central tropical Pacific Niño-4 region, where the teleconnections to the PNA pattern are more likely to originate through changes in deep convection (*e.g.,* Barsugli and Sardeshmukh, 2002; Alexander *et al.,* 2002). The figure shows that the Niño-4 SST anomalies for La Niña are in fact more consistently cold than El Niño conditions are consistently warm. This tropical asymmetry has also been discussed in previous studies (*e.g.,* Dommenget et al. 2013; Cai *et al.,* 2018). This result suggests that the teleconnections during La Niña would more consistently drive cold conditions in the CCS than

would El Niño events drive warm conditions, as found in our model response and in observations. This view is further substantiated by inspecting the histograms of meridional winds averaged over the CCS, shown in Figure 2.21 (bottom). As anticipated from the observed tropical Pacific Niño-4 SST asymmetry, the local winds are also more consistently upwelling favorable during La Niña conditions and less consistently downwelling favorable during El Niño conditions.

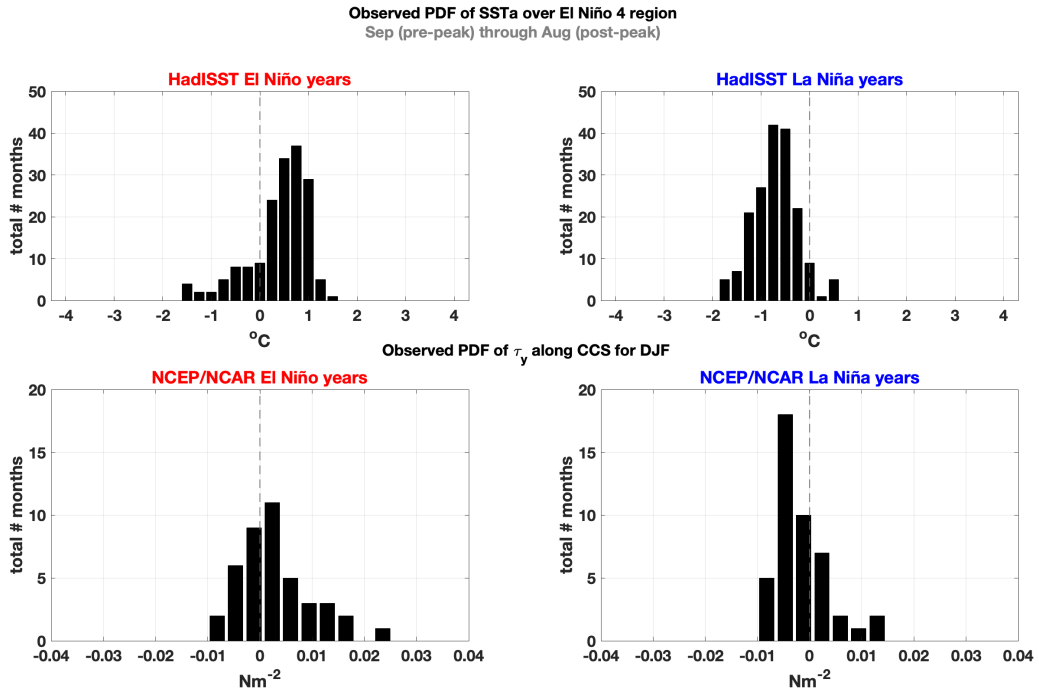

Figure 2.21 Histograms of observed SSTa during December-January-February over Niño-4 Region in the Tropical Pacific (top panels). Histogram of meridional wind stress over CCS for the same period (bottom panels). Observed warm events (μ=0.4, σ=0.61) have 79% of their months positive, while observed cold (μ=-0.7, σ=0.46) events have 94% of their months negative. Observed meridional CCS wind stress during warm events (μ=0.0027, σ=0.0071) have 64% of their months downwelling favorable, while cold events (μ=-0.0017, σ=0.005) have 71% of their months upwelling favorable.

Despite the model producing very weak chlorophyll values that are poorly correlated with the time-limited monthly-mean satellite surface observations, the model shows some skill in reproducing the timing of the climatology and the model better represents seasonal chlorophyll

variability in the northern region compared to the south. In contrast, the El Niño and La Niña composite vertically averaged chlorophyll response is more realistic in the southern parts of the CCS (cf. Thomas *et al.,* 2012). Composite zooplankton anomalies are essentially phase-locked to the chlorophyll field, upon which the zooplankton graze. This linear relationship is not surprising since the model only has one zooplankton group encompassing both microzooplankton and mesozooplankton, and so cannot represent the variety of populations in the CCS. Since the response of zooplankton to ENSO events varies by taxonomic group (Lilly and Ohman 2018), increased complexity in the modeled zooplankton is necessary to better represent zooplankton response to ENSO in the CCS. Improvements to marine ecosystem formulations via explicit representation of coastal species (*e.g.* Van Oostende *et al.* 2018) as well as interannually varying nutrient inputs (*e.g.,* surface runoff in the northern CCS, Hickey and Banas, 2008) could significantly improve the biogeochemical model skill in a forced ocean simulation. These types of model reformulations should be explored in future studies.

2.5. Conclusion

We show the composite variability of key physical and biogeochemical variables in the California Current System in the framework of the CESM-POP2-BEC model to develop a better understanding of the effects of ENSO on the oceanic ecosystem in that model. The 67-year long coarse-resolution ocean model simulation used for this study captures many of the expected main features related to ENSO events. The physical and biogeochemical processes in the simulation provide a comprehensive depiction of behavior of the system that cannot be obtained from observations alone. The simplicity of the composite approach makes it useful for determining the

physical changes driven by ENSO and ascertaining how these changes affect the ecological and biogeochemical state of the model system.

The results also give a measure of the predictable nature of the model system to forcing by ENSO. As the teleconnected response to remote ENSO events impacts the local oceanography of the CCS, the fidelity of predictions is reduced not only by deficiencies in the model but by local unpredictable processes in both the physics and biology as well. The coarse resolution model had significant errors in the physical response to forcing, which then cascaded into errors in the forcing that is provided to the ecosystem model. Higher-resolution physical-biogeochemical models will help to alleviate some of the model errors, but intrinsic variability in both physics and the ecosystem will further reduce the skill of linking ENSO variations to local physical-biological response. Quantification of these types of skill limits is the long-term goal of our research. These physical-biological composites provide a view of some of the limitations to the potentially predictable impacts of ENSO on the CCS in the framework of CESM-POP2-BEC.

Acknowledgements

This study forms a portion of the Ph.D. dissertation of NCQ, who was partially supported by a UC Mexus CONACYT Fellowship. The National Science Foundation (California Current Ecosystem-LTER, OCE1637632) and the National Oceanic and Atmospheric Administration (NOAA-MAPP; NA17OAR4310106) provided additional funding for this research. Many of the ideas pursued in this study were motivated by the scientists who attended the U.S. CLIVAR "Workshop on Forecasting ENSO Impacts on Marine Ecosystems of the US West Coast" held at SIO in 2016. We thank Matthew Long for granting access to the POP2-BEC simulation used in

this study, and for providing important feedback on the manuscript. We thank the four anonymous referees who provided extensive and insightful comments that significantly improved the clarity and interpretation of our results in this manuscript.

Chapter 2 is, in full, a reprint of the material as it appears in Ocean Modelling 2019 Cordero-Quirós, N., Miller, A.J., Subramanian A.C., Luo, J.Y., Capotondi, A., 2019. Composite physical-biological El Niño and La Niña conditions in the California Current System in CESM1-POP2-BEC. Ocean Modelling, 142, 101439. https://doi.org/10.1016/j.ocemod.2019.101439. The dissertation author was the primary investigator and author of this paper.

References

Alexander, M.A., Bladé, I., Newman, M., Lanzante, J.R., Lau, N.C., Scott, J.D., 2002. The atmospheric bridge: The influence of ENSO teleconnections on air-sea interaction over the global oceans. J. Clim. 15, 2205–2231.

An, S.I., Jin,F.F., 2004. Nonlinearity and asymmetry of ENSO. J. Clim. 17, 2399-2412.

Ashok, K., Behera, S.K., Rao, S.A., Weng, H., Yamagata,T., 2007. El Niño Modoki and its possible teleconnections. J. Geophys. Res. 112, C11007.

Bakun, A., Black, B.A., Bograd, S.J., Garcia-Reyes, M., Miller, A.J., Rykaczewski, R.R., Sydeman, W.J., 2015. Anticipated effects of climate change on coastal upwelling ecosystems. Current Climate Change Rep. 1, 85-93.

Barsugli, J. J., Sardeshmukh, P. D., 2002. Global atmospheric sensitivity to tropical SST anomalies throughout the Indo-Pacific Basin, J. Clim. 15, 3427-3442.

Bograd, S.J., Lynn, R.J. 2001. Physical-biological coupling in the California Current during the 1997-1998 El Niño-La Niña cycle. Geophys. Res. Lett. 28, 275-278.

Bograd, S. J., Lynn, R.J. 2002. Long-term variability in the Southern California Current System. Deep-Sea Research II 50, 2355-2370.

Burgers, G., Stephenson, D.B. 1999. The “normality” of El Niño. Geophys. Res. Lett. 26, 1027-1030.

Cai, W., Wang, G., DeWitte, B., Wu, L., Santoso, A., Takahashi, K., Yang, Y., Carréric, A., McPhaden, M.J, 2018. Increased variability of eastern Pacific El Niño under greenhouse warming. Nature 564, 201-206.

Capotondi, A., Wittenberg, A.T., Newman, M., Di Lorenzo, E., Yu, J.-Y., Braconnot, P., Cole, J., DeWitte, B., Giese, B., Guilyardi, E., Jin, F.-F., Karnauskas, K., Kirtman, B., Lee, T., Schneider, N., Xue, Y., Yeh, S-W., 2015. Understanding ENSO Diversity. Bulletin of the American Meteorological Society, 96 921-938

Capotondi, A., P. D. Sardeshmukh, E. Di Lorenzo, A. Subramanian and A. J. Miller, 2019. Predictability of US West Coast Ocean Temperatures is not solely due to ENSO. Scientific Reports, 9, 10993, doi.org/10.1038/s41598-019-47400-4..

Chávez, F. P., and Coauthors, 2002. Biological and chemical consequences of the 1997–1998 El Niño in central California waters. Prog. Oceanogr., 54, 205-232, doi:10.1016/S0079-6611(02)00050-2.

Chávez, F. P., and M. Messié. 2009. A comparison of Eastern Boundary Upwelling Ecosystems, Prog. Oceanogr., 83, 80–96, doi:10.1016/j.pocean.2009.07.032.

Checkley, D.M., Barth, J.A., 2009. Patterns and processes in the California Current System. Prog. Oceanogr. 84, 49–64.

Chelton, D.B., DeSzoeke, R.A., Schlax, M.G., El Naggar, K., Siwertz, N., 1998. Geographical variability of the first baroclinic rossby radius of deformation. J. Phys. Oceanogr. 28 (3), 433–460.

Chenillat, F., Rivière, P., Capet, X., Di Lorenzo, E., Blanke, B., 2012. North Pacific Gyre Oscillatino modulates seasonal timing and ecosystem functioning in the California Current upwelling system. Geophys. Res. Lett. 39 L01606, doi:10.1029/2011GL049966

Collins, C.A., Pennington, J.T.., Castro C.G., Rago, T.A., and Chávez, F.P. 2003. The California Current system off Monterey, California: physical and biological coupling. Deep-Sea Res. II, 50, 2389-2404.

Crawford, W.J., Moore, A.M., Jacox, M.G., Fiechter, J. Neveu, E., Edwards, C.A. 2017. A resonant response of the California Current circulation to forcing by low frequency climate variability. Deep-Sea Res. II 151, 16-36.

Crawford, W., 2017. *Investigations of the California Current System: Climate Variability and Advances in Modeling the Circulation*, Ph.D. Dissertation, UC, Santa Cruz, 224 pp.

Curchitser, E.N., H.P. Batchelder, D.B. Haidvogel, J. Fiechter, J. Runge (2013). Advances in physical, biological, and coupled ocean models during the US GLOBEC Program. Oceanography 26, 54-69

Danabasoglu, G., Bates, S.C., Briegleb, B.P. 2012. The CCSM4 Ocean Component. J. Climate, 25, 1361-1389, https://doi.org/10.1175/JCLI-D-11-00091.1

Deser, C., I. Simpson, A. Phillips, and K.A. McKinnon. How well do we know ENSO's climate impacts over North America, and how do we evaluate models accordingly? Journal of Climate, 31, 4991-5014.

Di Lorenzo, E., A. J. Miller, N. Schneider and J. C. McWilliams, 2005: The warming of the California Current: Dynamics and ecosystem implications. Journal of Physical Oceanography, 35, 336-362.

Di Lorenzo, E., K. M. Cobb, J. C. Furtado, N. Schneider, B. T. Anderson, A. Bracco, M. A. Alexander and D. J. Vimont, 2010. Central Pacific El Niño and decadal climate change in the North Pacific Ocean. Nature Geoscience, 3 762-765.

Di Lorenzo, E., V. Combes, J. E. Keister, P. T. Strub, A. C. Thomas, P. J. S. Franks, M. D. Ohman, J. C. Furtado, A. Bracco, S. J. Bograd, W. T. Peterson, F. B. Schwing, S. Chiba, B. Taguchi, S. Hormazabal and C. Parada, 2013. Synthesis of Pacific Ocean Climate and Ecosystem Dynamics. Oceanography, 26 68-81.

Di Lorenzo, E., and A. J. Miller, 2017. A framework for ENSO predictability of marine ecosystem drivers along the US West Coast. *US CLIVAR Variations*, 15, 1-7.

Dommenget, D., T. Bayr, and C. Frauen, 2013. Analysis of the non-linearity in the pattern and time evolution of El Niño Southern Oscillation. *Climate Dyn.*, 40, 2825–2847

Fiedler, P. C., & Mantua, N. J., 2017. How are warm and cool years in the California Current related to ENSO?. *Journal of Geophysical Research: Oceans*, *122*(7), 5936-5951, doi:10.1002/2017JC013094.

Fisher, J. L., W. T. Peterson, R. R. Rykaczewski. 2015. The impact of El Niño events on the pelagic food chain in the northern California Current. Global Change Biology, 21 4401-4414.

Franks, P. J. S., E. Di Lorenzo, N. L. Goebel, F. Chenillat, P. Riviere, C. A. Edwards and A. J. Miller, 2013. Modeling physical-biological responses to climate change in the California Current System. Oceanography, 26, 26-33.

Frischknecht, M., M. Munnich., Gruber, N. 2015. Remote versus local influence of ENSO on the California Current System. J. Geophys. Res. Oceans, 120, 1353-1374

Frischknecht, M., M. Munnich., Gruber, N. 2017. Local atmospheric forcing driving an unexpected California Current System response during the 2015-2016 El Niño, Geophys. Res. Lett., 44, 304–311

Frischknecht, M., M. Münnich and N. Gruber, 2018. Origin, Supply, Production and Fate: The three-dimensional Biological Pump in the California Current System, Journal of Geophysical Research- Oceans, 123, 7939–7962 .

Geider, R.J., MacIntyre, H.L., Kana, T.M., 1997. Model of phytoplankton growth and acclimation: responses of the balanced growth rate and the chlorophyll a: carbon ratio to light, nutrient-limitation and temperature. Mar. Ecol. Prog. Ser. 48, 187–200.

Geider, R. J., H. L. MacIntyre, and T. M. Kana,1998. A dynamic regulatory model of phytoplankton acclimation to light, nutrients, and temperature, Limnol. Oceanogr., 43, 679–694.

Gershunov, A, Barnett TP. 1998. ENSO influence on intraseasonal extreme rainfall and temperature frequencies in the contiguous United States: Observations and model results. Journal of Climate. 11,1575-1586.

Goebel, N.L., Edwards, C.A., Zehr, J.P., Follows, M.J., 2010. An emergent community ecosystem model applied to the California Current System. Journal of Marine Systems 83 221-241.

Griffies, S., Biastoch, A. Boöning, C., Bryan F., Danabasoglu G., Chassignet, E.P., England, M.H., Gerdes, R., Haak, H., Hallber, R.W., Hazeleger, W., Jungclaus, J., Large, W.G., Madec, F., Pirani A., Samuels, B., Sheinert, M., Gupta, A.S., Severijns, C.A., Simmons, H.L., Treguier, A.M., Winton, M., Yeager, S., Yin, J. 2009. Coordinated Ocean-ice Reference Experiments (CORE). Ocean Modelling, 26. 1-46.

Gruber, N., Lackhar, Z., Frenzel, H., Marchesiello, P., Münnich, M., McWilliams, J. C., Nagai, T., and Plattner, G.-K., 2011. Eddy-induced reduction of biological production in eastern boundary upwelling systems, Nat. Geosci., 4, 787–792, doi:10.1038/NGEO1273.

Hickey, B.M., 1998. Coastal oceanography of western North America from the tip of Baja California to Vancouver Island. In: Robinson, A.R., Brink, K.H. (Eds.), The Sea, The Global Coastal Ocean: Regional Studies and Syntheses. J. Wiley and Sons Inc, New York, pp. 345–391.

Hickey, B.M., and Banas, N.S, 2008. Why is the northern end of the California Current System so productive? Oceanography 21 90–107.

Hsieh, W., 1983. The free kelvin wave in finite-difference numerical models. J. Phys. Oceanogr. 13 (8), 1383–1397.

Hurrell, J.W., Holland, M.M, Gent P.R., Ghan, S., Kay, JE., Kushner, P.J. Marque, J.-F., Large, W.G., Lawrence, D., Lindsay, K., Lipscomb, W.H. Long, M.C., Mahowald, N., Marsh, D.R., Neale, R.B., Rasch, P. Vavrus, S. Vertenstein, M. Bader, D., Collings, W.D., Hack, J.J. Kiehl, J. Marshall, S. 2012. The Community Earth System Model: A framework for Colaborative Research. Bull. Amer. Meteor. Soc., 94, 1339-1360, https://doi.org/10.1175/BAMS- D-12-00121.1.

Jacox, M.G., Fiechter, J., Moore, A.M., Edwards, C.A., 2015. ENSO and the California Current coastal upwelling response. J. Geophys. Res. Oceans, 120, 1691-1702.

Jacox, M.G., et al., 2016. Impacts of the 2015–2016 El Nino on the California Current system: early assessment and comparison to past events. Geophys. Res. Lett. 43,7072–7080.

Jacox, M. G., M. A. Alexander, C. A. Stock, and G. Hervieux, 2017. On the skill of seasonal sea surface temperature forecasts in the California Current System and its connection to ENSO variability, Climate Dynamics, 1-15, doi:10.1007/s00382-017-3608-y.

Jahn, A., Sterling, K., Holland, M.M., Kay, J.E., Maslanik, J.A., Bitz, C.M., Bailey, D.A., Stroeve, J. Hunke, E.C., Lipscomb, W.H., Pollak, D.A. 2011. Late-Twentieth-Century Simulationof Arctic Sea Ice and Ocean Properties in the CCSM4. J. Climate, 25, 1431-1452, https://doi.org/10.1175/JCLI-D-11-00201.1

Kilpatrick, T., Xie, S-P., Miller, A.J., Schneider, N., 2018. Satellite Observations of enhanced chlorophyll variability in the Southern California Bight. J. of Geophys. Res. Oceans, 123, 7550–7563.

Kim, H.-J., Miller, A.J., 2007. Did the thermocline deepen in the souther California Current after the 1976-1977 climate regime shift? J. Phys. Oceanogr. 37, 1733-1739.

Kim, H.-J., Miller, A.J., McGowan, J., Carter, M.L. 2009. Coastal phytoplankton blooms in the Southern California Bight. Progress in Oceanography 82, 137-147.

Levine A.F.Z, Jin F.F., McPhaden, M.J., 2016. Extreme noise-extreme El Niño: How state-dependent noise forcing creates El Niño-La Niña asymmetry. J Clim.
29 5483-5499.

Large, W.G., Yeager, S., 2009. The global climatology of an interannually varying airsea flux data set. Clim. Dyn. 33, 341–364

Lilly, L. and Ohman, M. 2018. CCE IV: El Niño-related zooplankton variability in the southern California Current System. Deep-Sea Res. 120, 36-51.

Lynn, R.J., and Simpson, J.J. 1987. The California Current System: The Seasonal Variability of tis Physical Characteristics. J. of Geophys. Res. 92, 947-966.

McGowan, J. A., D. R. Cayan, and L. M. Dorman, 1998. Climate-ocean variability and ecosystem response in the northeast Pacific. Science, 281, 210–217.

McGowan, J.A., Bograd, S.J., Lynn, R.J., Miller, A.J., 2003. The biological response to the 1977 regime shift in the California Current. Deep-Sea Res. 50, 2567-2582.

McPhaden, M.J., Busalacchi, A.J., Cheney, R., Donguy, J.-R., Gafe, K.S., Hapern, D., Ji, M., Julian, P., Meyers, G., Mitchum, G.T., Niiler, P.P., Picaut, J., Reynolds, R.W., Smith, N., Takeuchi, K., 1998. The Tropical Ocean-Global Atmopshere observing system: A decade of progress. J. Geophys. Res. 103, 14,169-14,420.

Miller. A.J., Song, H., Subramanian, A.C., 2015. The physical oceanographic environment during the CCE-LTER Years: Changes in climate and concepts. Deep-Sea Res. 112, 6-17.

Moore, J. K. J., Doney, S. C., Lindsay, K. 2004. Upper ocean ecosystem dynamics and iron cycling in a global three-dimensional model. Global Biogeochemical Cycles, 18, GB4028 doi:10.1029/2004GB002220.

Moore, J. K., Doney, S., Kleypas, J., Glover, D., and Fung, I., 2002. An intermediate complexity marine ecosystem model for the global domain, Deep-Sea Res. II, 49, 403-462.

Moore, J. K., Lindsay, K., Doney, S.C., Long, M.C., Misumi, K. 2013. Marine Ecosystem Dynamics and Biogeochemical Cycnling in the Commnunity Earth System Model [CESM1(BGC)]: Comparison of the 1990s with the 2090s under the RCP4.5 and RECP8.5 Scenarios. J. Climate, 26, 9291-9312 https://doi.org/10.1175/JCLI-D-12-00566.1.

Niebauer, H.J. 1988. Effects of El Niño-Southern Oscillation and North Pacific weather patterns on interannual variability in the subarctic Bering Sea. J. Geophys. Res., 93, 5051-5068.

Newman, M., M. A. Alexander, T. R. Ault, K. M. Cobb, C. Deser, E. Di Lorenzo, N. J. Mantua, A. J. Miller, S. Minobe, H. Nakamura, N. Schneider, D. J. Vimont, A. S. Phillips, J. D. Scott, C. A. Smith, 2016. The Pacific Decadal Oscillation, revisited. Journal of Climate, 29, 4399-4427.

Ohman, M. D., 2018. Introduction to collection of papers on the response of the southern California Current Ecosystem to the Warm Anomaly and El Niño, 2014–16, Deep-Sea Res., 140, 1-3.

Ohman, M. D., K. Barbeau, P. J. S. Franks, R. Goericke, M. D. Landry, A. J. Miller, 2013. Ecological transitions in a coastal upwelling ecosystem. Oceanography, 26, 210-219.

O'Reilly, J.L., Maritorena, S., O'Brien, M.C., Siegel, D.A., Toole, D., David Menzies, D., Smit R. C., J.E., Mueller, Mitchell, B.G., Kahru , M., Chavez, S.P., Strutton, P., Cota, G.F., Hooker, S.B., McClain, C.R., Carder, K.L., Müller-Karger, F., Harding, R., Magnuson, A., Phinney D., Moore, G.F., Aiken, J., Arrigo, K.R., Letelier, R., Culver, M., 2000. SeaWiFS Postlaunch Calibration and Validation Analyses, Part 3. NASA Tech. Memo. 2000-206892, Vol. 11, S.B. Hooker and E.R. Firestone, Eds., NASA Goddard Space Flight Center.

Rayner, N.A., Parker, D.E., Horton, E.B., Folland, C.K., Alexander, L.V., Rowell, D.P. 2003. Global analyses of sea surface temperature, sea ice, and night marine air temperature since the late nineteenth century. J. Geophys. Res., 108, 4407, doi:10.1029/2002JD002670.

Rudnick, D. L., K. D. Zaba, R. E. Todd, and R. E. Davis, 2017. A climatology of the California Current System from a network of underwater gliders. Progress in Oceanography, 154, 64-106.

Schwing, F.B., Palacios, D.M., and Bograd, S. J., 2005. El Niño impacts on the California Current ecosystems. U.S. CLIVAR Newsletter, Vol. 3, No. 2, 5-8.

Small, J., Curchitser, E., Hedstrom, K., Kauffman, B., and Large, W. 2015. The Benguela Upwelling System: Quantifying the Sensitivity to Resolution and Coastal Wind Representation in a Global Climate Model. J. Climate. 28, 9409-9432.

Song, H., A. J. Miller, B. D. Cornuelle and E. Di Lorenzo, 2011. Changes in upwelling and its water sources in the California Current System driven by different wind forcing. Dynamics of Atmospheres and Oceans, 52, 170-191.

Thomas, A. C., Brickley, P., & Weatherbee, R., 2009. Interannual variability in chlorophyll concentrations in the Humboldt and California Current Systems. Progress in Oceanography, 83, 386–392.

Thomas, A. C., Strub, P. T., Weatherbee, R. A., & James, C., 2012. Satellite views of Pacific chlorophyll variability: Comparisons to physical variability, local versus nonlocal influences and links to climate indices. Deep-Sea Research Part II, 77-80, 99–106.

Turi, G., Alexander, M., Lovenduski, N., Capotondi, A., Scott, J., Stock, C., Dunne, J., John, J., and Jacox, M., 2018. Response of Oxygen and PH to ENSO of the California Current System in a high-resolution global climate model. Ocean Sci., 14, 69-86.

Van Oostende, N., Dussin, R., Stock, C.A., Barton, A.D., Curchitser, E., Dunne, J.P., and Ward, B.B. 2018. Simulating the ocean's chlorophyll dynamic range from coastal upwelling to oligotrophy. Progress in Oceanography. 168, 232-247. doi: 10.1016/j.pocean.2018.10.009.

Wang, H., Kumar, A., and Wang, W., Jha, B. 2012. U.S. Summer Precipitation and Temperature Patterns Following the Peak Phase of El Niño. Journal of Climate, 25, 7204-7215.

Chapter 3

Physical-Ecological Response of the California Current System to ENSO events in ROMS-NEMURO

Abstract

We analyze the bottom-up ENSO-driven physical-biological response of the CCS and the CCE in a high-resolution, "eddy-scale" ocean model with multiple classes of phytoplankton and zooplankton. The response of the SSTa is consistent with the asymmetries found in Chapter 2, with La Niña events being more consistently cold than El Niño events are consistently warm. The biogeochemical and ecological response is represented by ENSO-composite anomalies, lag-correlations with an ENSO index, and PDFs for ENSO years. The results show lower trophic level interactions during El Niño and La Niña events in which the larger components (diatoms, euphausiids, and copepods) are suppressed in the coastal upwelling zones during El Niño, while the smaller components (flagellates and ciliates) are enhanced. In addition, standing eddies of the CCS modulate the latitudinal structure of the ecological response to ENSO. The results point towards future research to understand how bottom-up changes may lead to variability of patterns in fish populations and top predators.

3. 1 Introduction

In our previous research (Chapter 2; Cordero-Quirós et al., 2019), we showed the abilities and limitations of a coarse-resolution, "climate-scale" ocean model in representing the physical-biological response in the California Current to ENSO variability. The coarse (~100km) resolution caused many aspects of the model response to be weak, poorly organized, and spread out over much larger areas than observations. In particular, upwelling dynamics along the coast

was incorrectly represented because the model grid spacing was larger than the local Rossby deformation radius.

Here we examine a much higher resolution, "eddy-scale" ocean model that is similarly forced with observed winds over many decades. The high (~7km) resolution allows proper representation of upwelling fronts along the irregular coastline as well as the generation of an energetic and unstable mesoscale eddy field over realistic topography. The ecological model is more sophisticated in that it includes two size classes of phytoplankton and three size classes of zooplankton. The model biogeochemistry, in contrast, is less sophisticated in that it includes only two nutrients (nitrate and silicate) and excludes the carbonate cycle. An added feature for this simulation is the inclusion of a small pelagic fish model that includes sardines and anchovies, plus a predator fish and fishing fleet, that is constructed in a Lagrangian formulation.

The basic state of the spatial distributions of phytoplankton communities, and the dependent zooplankton communities that feed on them and each other, establishes biogeographical regions across and along the CCS in the presence of complicated coastline variations and inhomogeneous eddy fields. We consider here how the local physical and ecological response of the CCS is perturbed by ENSO forcing in this context. We focus on individually analyzing the two phytoplankton groups and three zooplankton groups to provide a more fine-scaled view of the bottom-up response of the CCE to ENSO compared to the less sophisticated coarse-resolution model. The results reveal coherent responses for both warm and cold events, in spite of the mesoscale eddy "noise", and some interesting and surprising features in the ecology.

We first explain the basic framework of the physical and ecological models. Then we introduce our methods for statistical analyzing the system. We follow that with a presentation of results, and a summary and conclusion section.

3.2 Model Framework

3.2.1 Regional Ocean Circulation Model

The physical fields used for this analysis are from a simulation using the Regional Ocean Modeling System (ROMS; Haidvogel et al., 2008; Shchepetkin and McWilliams, 2005) that was executed by scientists at Rutgers University who generously provided us with the model output. The study domain spans the zonal extent of the CCS, roughly 1200 km offshore, from Vancouver Island (50ºN) to southern Baja California (20ºN), over a grid with 1/15º (~7 km) horizontal resolution (Van Oostende et al., 2018). The air-sea fluxes are computed using the Coordinated Ocean-Ice Reference Experiment (CORE; Griffies et al. 2009) protocol using observed reanalysis 6-hourly fields from 1958-2007 for the atmospheric variables and model SST. Boundary and initial conditions for temperature, salinity, and velocity are monthly values from the Simple Ocean Data Assimilation (SODA) model output (version 2.1.6), and atmospheric forcing is from the Modern Era Retrospective-analysis for Research and Applications (MERRA) reanalysis products (Van Oostende et al., 2018). Vertical mixing of momentum and tracers is performed along a vertical grid of 50 terrain-following surfaces (Van Oostende et al., 2018). Daily model fields were averaged into monthly means for all model variables for the full model time period from Jan 1959 to December 2007. Climatological

monthly mean averages were then formed and subtracted from the monthly means to obtain 1959-2007 monthly anomalies.

3.2.2 Ecosystem model

The ecological model is called NEMURO (North Pacific Ecosystem Model for Understanding Regional Oceanography; Kishi et al., 2007) and was developed by PICES CCCC (North Pacific Marine Science Organization, Climate Change and Carrying Capacity Program) as a prototype model to represent the basic trophic structure of the marine ecosystem components in the North Pacific. This lower trophic level nutrient-phytoplankton-zooplankton-detritus (NPZD) model has eleven state variables: nitrate (NO_3), ammonium (NH_4), small phytoplankton (PS), large phytoplankton (PL), small zooplankton (ZS), large zooplankton (ZL), predatory zooplankton (ZP), silicic acid ($Si(OH)_4$), and three detrital pools represented by dissolved organic nitrogen (DON), particulate organic nitrogen (PON), and particulate organic silicate (Opal). The PS and PL groups use parameters that represent flagellates and diatoms, respectively. ZP uses parameters that correspond to euphausiids (or krill) that feed on the mesozooplankton group PL (parameters for copepods), the microzooplankton group ZS (parameters for ciliates), as well as diatoms (PL). The copepods feed on both the diatoms (PL) and the flagellates (PS) as well as the ciliates (ZS). The ciliates (ZS) feed only on the flagellates (PS). The three zooplankton groups were also preyed upon by the modeled sardine and anchovy populations (discussed next). NEMURO uses nitrogen as its primary "currency", but also includes silicon as a limiting nutrient for diatoms. All the state variables are tracked in units of mmol N m^{-3}. The full details and balance equations of NEMURO are given in Kishi et al., 2007.

3.2.3 Individual-based fish model

The analyzed simulation also has a component that includes an individual-based model (IBM; Rose et al., 2015) representing two coastal pelagic species, anchovy, which prefers inshore conditions, and sardine, which prefers offshore conditions. There is also a migratory predator species, albacore, that consumes the two small pelagics, and a fishing fleet model that harvests only sardines. These small pelagic fish graze on zooplankton according to their feeding preferences from the NEMURO model fields. The IBM submodel tracks individuals of each of the three fish species along the ROMS grid. The life cycle of sardines and anchovies is divided into 6 life stages: egg, yolk-sac larval, larval, juvenile, subadult, and adult (Politikos et al., 2018). Each population is represented by Lagrangian particles that move through the Eulerian domain by advection and/or by swimming. Each particle can transition through the life stages as time passes, or die by grazing or senescence. Both sardines and anchovies are resolved with 10,000 particles each, while albacore and fishing boats each are allocated only 100 particles (Rose et al., 2015, Fiechter et al., 2015).

3.3 Composite analysis method

In order to isolate the ENSO signal and remove the impact of long-term trends and decadal climate variability, monthly mean anomalies for all ROMS fields were first high-pass filtered using Lanczos method with a cut-off frequency of 10 years, following Cordero-Quiros et al. (2019). Identification of El Niño and La Niña years then follows the NOAA protocol as explained in Chapter 2, and the composites for each month of the ENSO cycle, from September to August over the wintertime peak of each event, were computed using the same method (Cordero-Quirós et al., 2019).

The years from the ROMS-NEMURO simulation time period included in the 12-month El Niño composite are: 1963-1964, 1965-1966, 1968-1969, 1972-1973, 1982-1983, 1986-1987, 1987-1988, 1991-1992, 1994-1995, 1997-1998, and 2002-2003. The resulting years for the La Niña composite are: 1970-1971, 1971-1972, 1973-1974, 1975-1976, 1983-1984, 1984-1985, 1988-1989, 1995-1996, 1998-1999, 1999-2000. That yields a total of 11 El Niño events, and 10 La Niña events.

All of the composite variables were tested for significance using a simple bootstrap test at a 90% significance level and the grid locations where the composite variability is above this threshold are marked with black dots in the figures. Rather than showing all the composite months, like we showed in Chapter 2, in the following section, we only focus on key months of the composites and key lag relationships between variables. For this analysis, the nitrate was averaged from 25m to 100m, and the other NPZ model ecological variables were averaged from the surface to 100m.

3.4. Results

3.4.1 SST

The SSTa warming of the CCS associated with El Niño events during winter (DJF 3-month composite average), when the ENSO teleconnections peak, is shown in Figure 3.1 for the ROMS simulation and HadISST observations (Rayner et al., 2003). Composite winter model and observations both show that the warming of the CCS in response to El Niño tends to be significant only along a narrow band along the shore, and the warming signal weakens and becomes cool far offshore. Both the model and observations show the most intense warming off the coast of south Baja California and in the northern portion of the CCS. The near-coastal

signature suggests that the response to El Niño is tightly linked to the coastal dynamics controlled by the weakening of the upwelling winds during El Niño that lead to muted upwelling and consequent warming of the SSTa.

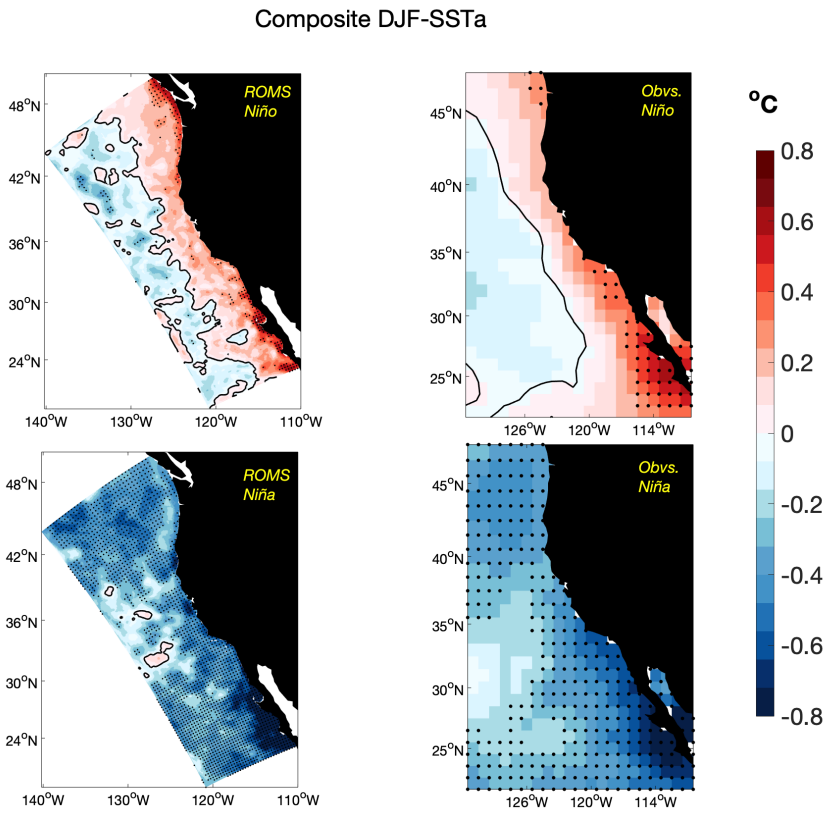

Figure 3.1 Composite DJF-average of SSTa for El Niño years (top) and La Niña years (bottom) for both ROMS and HadISST observations. Significant locations are marked with black dots.

Figure 3.1 also shows the composite DJF SSTa response of the CCS during cold events associated with La Niña. In contrast with El Niño, La Niña is associated with statistically significant cooling over nearly the entire domain of the CCS. The coldest anomalies tend to be at the southern and northern portions of the CCS, comparable to the patterns shown by El Niño-related SSTa, but they extend further offshore where they are consistently cool. This key difference in the consistency of the offshore response to El Niño and La Niña that is captured by

both coarse and fine resolution is not affected by the introduction of mesoscale activity, indicating that its origin lies in the large-scale dynamical response to atmospheric forcing.

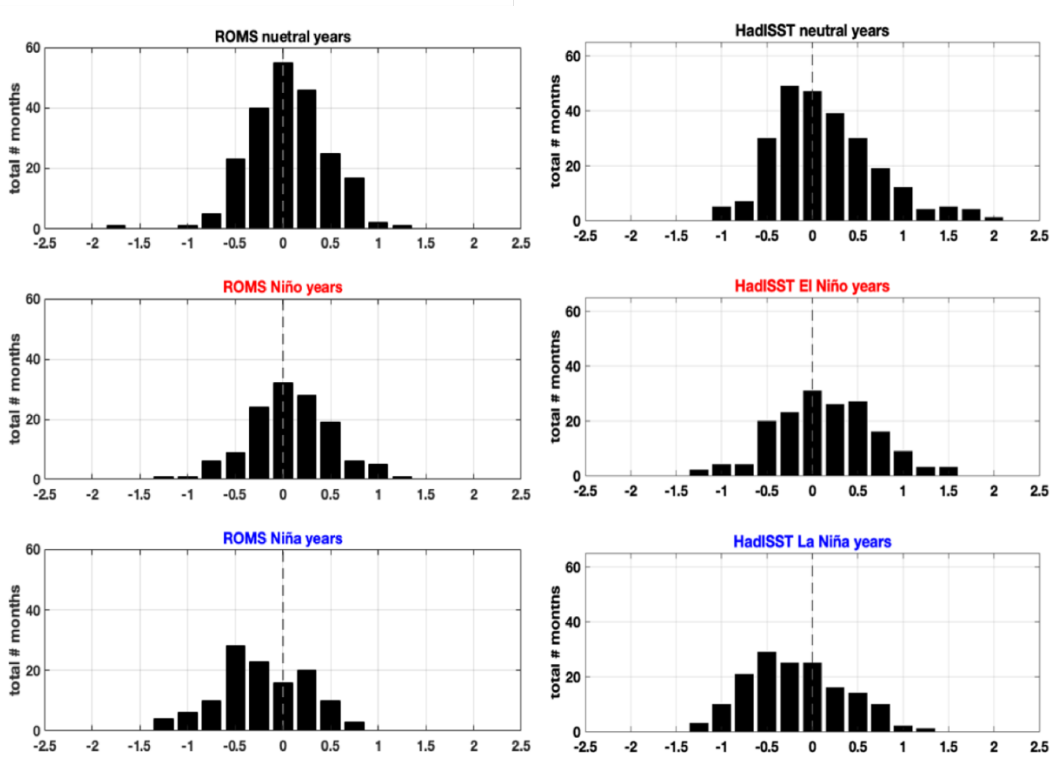

Figure 3.2 Histograms of modeled (left) and observed (right) SSTa during a 12-month period from September through August over the CCS for neutral, El Niño, and La Niña years.

The asymmetry between warm and cold events that was seen in the coarse resolution model also occurs in this high-resolution simulation. Figure 3.2 shows the probability distribution functions (PDFs) of monthly mean SSTa averaged over the model domain as captured by the ROMS and observations during a 12-month period from September through August for warm, cold, and neutral ENSO conditions. The PDFs show that in the model (Fig. 3.2, left) the SSTa during neutral and El Niño years tend to be relatively symmetric around the origin, so that cold anomalies also frequently occur during El Niño (only 57% of the SSTa are positive during warm events). In contrast, the PDF of model SSTa during La Niña shows a more consistent cooling of the CCS during those years, with much less frequent occurrences of warm

months (67% of SSTa are cold). Observations are generally consistent with the asymmetry of the model PDFs, with 55% of El Niño event anomalies being warm and 64% of the La Niña anomalies being cool. But observations also exhibit stronger anomalies in the PDFs. For example, observed neutral years appear to be strongly 'tailed' towards warm events, a feature that is not captured by the model. These differences may suggest possible model biases, be due to the mismatch of air-sea coupling on the eddy scale due to the forcing protocol (e.g., Seo et al., 2016), or be associated with the random mesoscale activity that occurs differently in the model and observations. Overall, these results further confirm the asymmetrical response of the CCS in which La Niña events are associated with a more consistent cooling than El Niño events are associated with consistent warming (cf., Fiedler and Mantua, 2017), even though El Niño is associated with the most extreme warm SSTa events (e.g., McGowan et al., 1998).

3.4.2 Lower trophic level response

We next explored the relationship of the nutrients, phytoplankton and zooplankton fields to the changes in ENSO conditions. Nitrate and small phytoplankton show a coherent response in winter but all of the ecological fields showed their largest and most significant ENSO response in the spring season when their seasonal bloom occurs. This is in contrast to the physical response that peaks significantly in late winter after the atmospheric teleconnection forcing has generated its largest oceanic signal. Rather than showing the composite maps of all the ecological variability, for brevity we first show the map for JFM 3-month composite average anomalies of nitrate (which is also representative of the spring), and then present the lagged correlation between the wintertime ENSO index (ONI) and the springtime ecological response.

The structures seen in these correlation maps are very similar to those seen in the various composite maps, which are remarkably persistent from month to month in the spring.

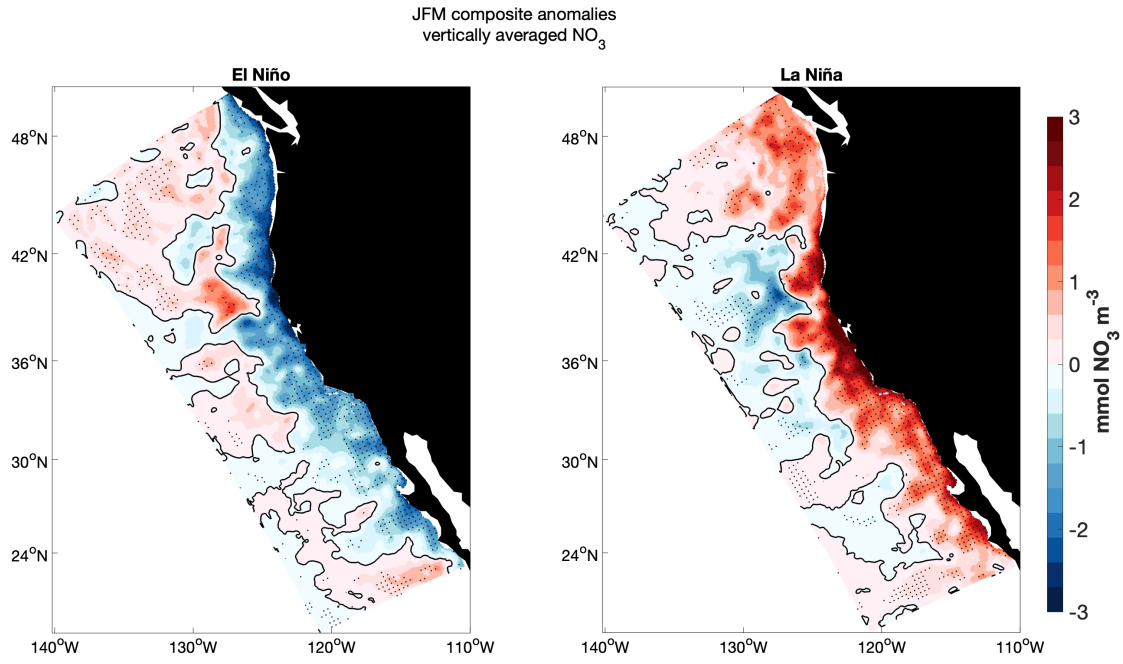

Figure 3.3 Composite JFM-averaged anomalies of vertically averaged (25m to 100m) NO_3 for El Niño (left) and La Niña (right) years. Locations where composite response is significant are marked every 5 grid points (black dots).

3.4.3 Composite variability of NO_3

The biogeochemical response of the CCS during warm and cold events is succinctly represented by composite anomalies of nitrate (NO_3) concentrations in the water column (averaged from 25 to 100 m) during JFM. Similar results hold for the silicate field. Figure 3.3 shows that the composite vertically averaged anomalies of NO_3 in the model captures the nutrient depleted conditions along the coast due to muted coastal upwelling during El Niño, and nutrient enhancement due to stronger upwelling during La Niña. The spatial distribution of ENSO-related composite NO_3 anomalies is confined to a roughly 500km region along the coast, with more patchy structure offshore during both warm and cold events. Unlike composite SSTa, the

composite anomalies of NO_3 are quite symmetric over the CCS in both their spatial pattern and significance, except for slight differences off Southern California Bight and Baja California. The upwelling-driven response of the NO_3 in the water column may be further amplified by changes in the biogeochemistry of the source waters (Rykaczewski and Dunne, 2010; Bograd et al., 2015) but further research is necessary to address this issue.

3.4.4 Lagged correlation of lower trophic levels with the ONI

Figure 3.4 shows the 3-month lagged correlation between January ONI values and April anomalies of the ecological fields in NEMURO. Positive values (red) indicate that biomass anomalies during April over the CCS are in phase with the SSTa in January over the tropical Pacific. During El Niño conditions over the CCS when upwelling favorable winds tend to be weaker, the nutrient supply to the photic zone decreases, as shown by the negative lagged-correlations of vertically averaged NO_3 (which is similar to the silicate fields) along the coastal region. As a consequence of the nutrient-depleted waters, large phytoplankton (diatom) biomass decreases along the coastal band and in patchy areas offshore. The response of the predatory zooplankton (krill) and mesozooplankton (copepods) that each graze partly on diatoms resembles this diatom field. The predatory zooplankton has a stronger correlative response to ONI than mesozooplankton since it preys upon the now-reduced field of mesozooplankton. Thus, the larger components of the food web respond as expected with reductions in biomass for El Niño conditions and enhancements for La Niña conditions.

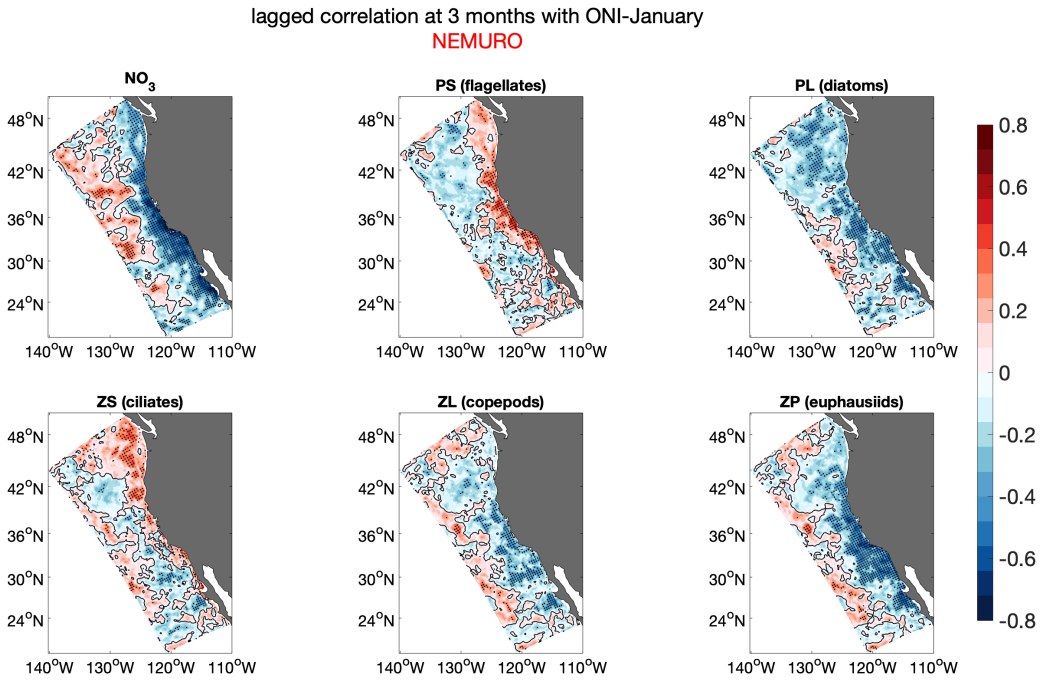

Figure 3.4 Lagged correlation of ecological fields during April with January of the Oceanic Niño Index (ONI). Locations where correlations are >95% confidence level are marked with black dots.

In contrast, along the coastal region Figure 3.4 shows that positive anomalies of small phytoplankton (flagellates) biomass occur during warm event conditions (positive ONI). This is consistent with smaller phytoplankton cells having lower nutrient requirements and more effective uptake, which gives them competitive advantage over larger cells (diatoms) under low nutrient conditions (Van Oostende et al., 2018; Edwards et al., 2012). Small zooplankton (ciliates) also increases in these near-coastal areas, both due to the enhancement to its only food source (the flagellates) and to the reductions in both of its predators (euphausiids and copepods). Figure 3.4 clearly shows that NEMURO captures this kind of ecosystem dynamics where the smaller phytoplankton groups thrive under lower nutrient conditions nearshore due to muted upwelling during El Niño. This type of response to El Niño, where there are winners in the smaller components of the food web near the coast, is an unexpected result of our analysis and

shows the efficacy of adding more complexity to the food web compared to the ecological model results in Chapter 2.

Another interesting feature of the ecological correlation maps (and seen consistently in the month-to-month composite response as well, as in Figure 3.3) is the occurrence of ecological anomalies locked spatially around standing eddies (also called permanent meanders or stationary waves) in the simulated California Current. These have been previously discussed for the physical fields of currents and sea level (Marchesiello et al., 2003; Centurioni et al., 2008), but we have not noticed this type of response being linked so clearly to the ecology, especially in the context of modulation of the ecological fields by ENSO. The large-scale standing eddies (roughly four of them, undulating north-south along the CCS) are locked to major capes and bathymetric features and are also associated with local enhancements of the mesoscale eddy field. They might be channels for filament ejection of biomass from coastal regions, whereby strong production near the coast is transported offshore by the eddies or the mean flow. This result needs to be further explored in future work to establish the dynamical drivers of the structures of the ecological response and its modulation by ENSO.

3.4.5 Probability distribution of ecological fields over the CCS

In order to address differences in the consistency of the ecological response of the CCE to cold and warm events, we computed PDFs of the ecological fields in NEMURO over a coastal swath from 22^{o} N to 48^{o} N extending roughly 300 km offshore, which is the region of strongest response to ENSO seen in the composites. The PDFs of NO_3 anomalies show a fairly consistent depletion during El Niño years with fairly consistent enhancement of NO_3 during La Niña

(Figure 3.5). Negative anomalies represent 71% of the total distribution for El Niño years, and 77% of the anomalies are positive for La Niña years, which is much more symmetric than found for the SSTa PDFs.

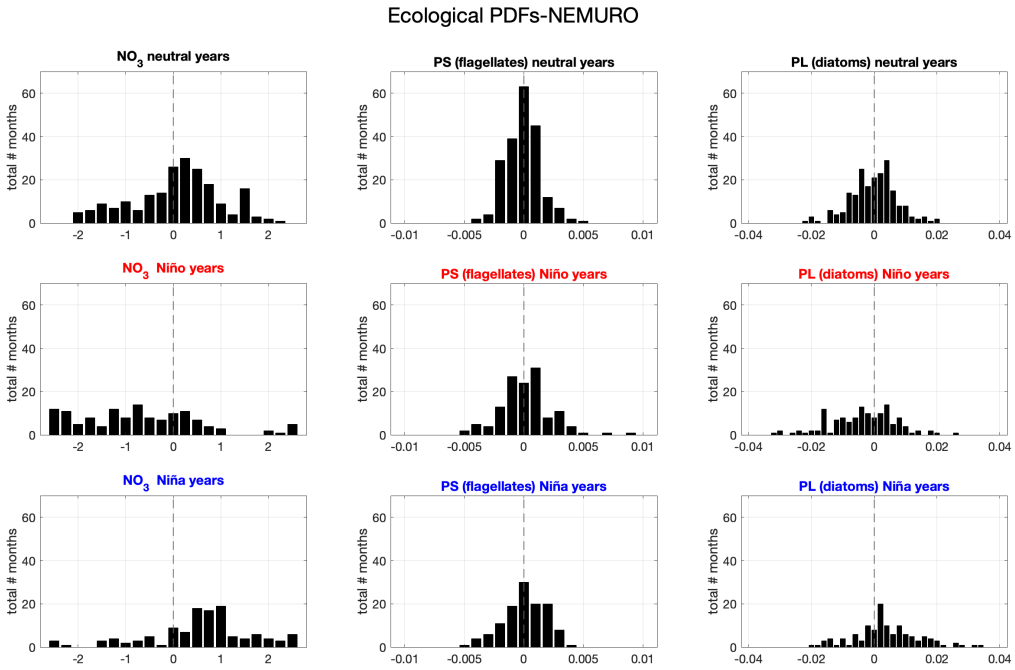

Figure 3.5 Histograms of anomalies vertically averaged NO_3 (left), small phytoplankton (middle), and diatoms (right) during a 12-month period from September through August over a coastal swath of ~300 off-shore from 22° N to 48° N.

PDFs for diatoms, in contrast, have more consistency during cold events, with 70% of negative anomalies during La Niña and 59% of positive anomalies during El Niño (Figure 3.5). The ciliates, however, are less consistently altered (Figure 3.5) than diatoms for both warm (49%) and cold events (57%) indicative of their narrower coastal response and higher signals in the high latitudes (see Figure 3.4). The distribution for predatory zooplankton (Figure 3.6) is less consistent than for diatoms, with El Niño (La Niña) events having 64% (70%) of their associated anomalies on the negative (positive) side of the distribution. Similar results hold for the copepod distributions (50% vs. 69%). And the ciliates reflect the flagellate distribution (47% vs. 63%) but

with a stronger consistency during La Niña events. The percentage of cold and warm anomalies associated to each event for every ecological group and SST are summarized in Table 3.1. In general, the PDFs of the biological fields in NEMURO do not exhibit such a strong asymmetry as that associated with SSTa. This suggests more complicated dynamics that go beyond a linear response to wind variability imprinted by ENSO teleconnections.

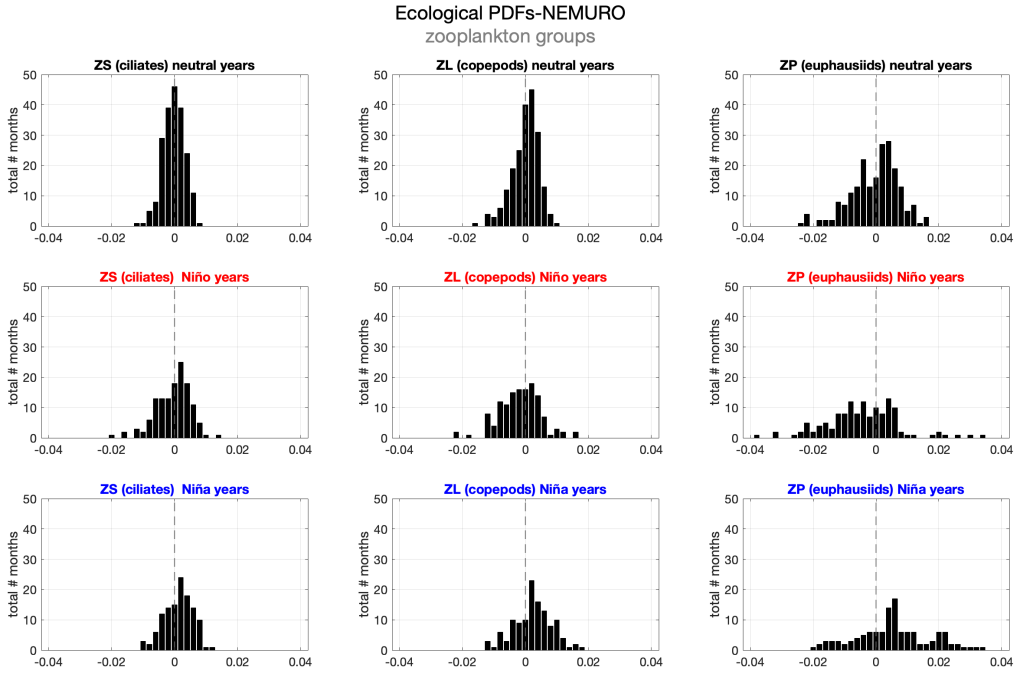

Figure 3.6 Histograms of anomalies of small zooplankton (left), large zooplankton (middle), and predatory zooplankton (right) during a 12-month period from September through August over a coastal swath of ~300 off-shore from 22° N to 48° N.

TABLE 3.1 Percentage of warm anomalies during El Niño years (second column) and of cold anomalies during La Niña years (last column) for ecological variables and SST.

	EN<0 (%)	LN>0 (%)
NO_3	71	77
PS	49	57
PL	59	70
ZS	47	63
ZL	58	69
ZP	64	70
SST ROMS	57	67
SST HadISST	55	64

3.4.6 Fish IBM

We made an attempt to analyze the fish IBM to assess whether ENSO changes in the environment can drive changes in characteristics of the sardine and anchovy populations in variables such as egg counts, larval survival, juvenile growth, and adult preferred habitat (e.g., Sánchez-Garrido et al., 2020). However, our analysis was hampered by several factors. For example, an examination of the IBM particle counts assigned to each life stage of the small pelagics over the course of the simulation revealed problems with the assigned particle counts exhibiting long-term trends and unphysical arbitrary resets. Also, long-term trends in adult fish populations (Politikos et al., 2018) appeared to overwhelm any strong ENSO signals in their response, suggesting that a long-term spin-up of the fish models into a "statistical equilibrium" might be required. We did note several interesting features of how the numerical strategy of assigning life stages to particles related to daily-to-monthly-to-yearly life-stage transitions (characteristics that are assigned in the code parameters). However, a detailed analysis of this IBM fish model in the context of ENSO variability will require extensive future research.

3.5. Summary and Conclusion

We analyzed the bottom-up ENSO-driven physical-biological response of the CCS and the CCE in a high-resolution, "eddy-scale" ocean model with two classes of phytoplankton and three classes of zooplankton. The physical oceanographic responses in SSTa exhibited asymmetries similar to those in the coarse resolution model found by Cordero-Quirós et al. (2019), with La Niña events being more consistently cold than El Niño events are consistently warm (Figures 3.1 and 3.2). We used a statistical analysis strategy involving composites, lag correlations, and PDFs to assess the ENSO-forced biogeochemical and ecological response (Figures 3.3-3.5). We found that the larger components (diatoms, euphausiids, and copepods) are suppressed in the coastal upwelling zones during El Niño, while the smaller components (flagellates and ciliates) are enhanced.

Most observational studies of the ecological response to ENSO in this region aggregate phytoplankton and zooplankton, so it is unclear how realistic this simulation is. In general, chlorophyll is often used as a proxy for phytoplankton biomass. An example of this is the BEC model used in the previous chapter to composite the response of chlorophyll during ENSO events. This approach facilitates comparison with satellite observations of chlorophyll (e.g., Thomas et al., 2012). The type of algorithms that are used for chlorophyll computation involve variables that are unique to each phytoplankton size-class e.g., grazing and mortality rates, and saturation constants for nutrient uptakes. Thus, using chlorophyll as a proxy for phytoplankton biomass may provide a decent broad-brush view of the response of the ecosystem to ENSO, but the complexity of its calculation can obscure the dynamics at lower trophic levels.

The dichotomy in the details of the simulated bottom-up response of the CCE to ENSO (Fig. 3.4) motivates us to identify interactions between the lower trophic levels. When El Niño drives nutrient depletion in the photic zone due to suppressed upwelling, the larger phytoplankton (diatoms) has less nutrients available for their uptake and growth, resulting in decreased biomass. It is unclear whether the decrease in diatoms biomass is dominated by mortality or by reduced size as a consequence of nutrient limitation, but future research could analyze the changes in opal detrital pool in order to address this question. Small phytoplankton is more resilient to nutrient depletion since its size allows for smaller nutrient concentrations, and at the same time they face less competition from diatoms for nutrients. During La Niña, intensified upwelling brings nutrients to the photic zones favoring phytoplankton populations, particularly the larger ones with more capacity for uptake. Once more, competition comes into play, and small phytoplankton is reduced under upwelling favorable conditions.

The results also show that vertically averaged concentrations of NO_3 in the water column increase in response to intensified upwelling during La Niña and decrease as a consequence of weaker upwelling during El Niño (Figs. 3.3-3.5). If we consider the alongshore winds stress along the CCS to be the primary driver of coastal upwelling and consequent nutrient supply, one could expect the NO3 response to be as asymmetrical as the SSTa. Nevertheless, the lack of this asymmetry suggests that other dynamics come into play when determining the ENSO related variability of NO_3. The supply of nutrients to the photic zone is also determined by subsurface ocean variability e.g., pycnocline depth and chemical properties of the source waters. Future analysis of the subsurface conditions is necessary to understand the local and advective changes

that impact the supply of NO3 into the photic zone, and how these conditions change in response to ENSO.

The coarse resolution of the global circulation model of Chapter 1 does not account for the many interesting effects of mesoscale eddy features that drive variability in the EBUS like the CCS. For example, we noted a fascinating structure in the ecological response that is linked to the latitudinal structure of the standing eddies, and possibly the mesoscale eddy distribution, locked into the CCS. This response structure is clearly evident in the composites (Figure 3.3) and in the correlation maps (Figure 3.4), which suggests a linear modulation of the background flow fields between El Niño and La Niña events. It is still unclear how the mesoscale features of the CCS drive an influence the variability of the biogeochemical properties of the CCE, and how this may further impact the spatial distribution of phytoplankton and zooplankton communities, both under normal conditions and during ENSO events. Patterns of fish migration highly depend on the regions of high nutrient concentration, and fish catch is strongly related to high chlorophyll coastal regions (Stock et al., 2017). Future work is needed in order to shed light on these dynamics. This will help us better address the future changes of habitat of fish populations like sardine and anchovy, as well as top predators, as a response of changes in their environmental modulators on seasonal, interannual and global warming timescales.

In conclusion, we found that the asymmetries in the response of the CCS to ENSO events are also captured by the high-resolution model used in this chapter. It is noteworthy how a simple lower trophic level NPZD model like NEMURO is a useful tool to represent the bottom-up ENSO related response of the CCE. The ecological model allows to identify key interactions

between large (diatoms) and small (flagellates) phytoplankton groups and their corresponding zooplankton grazers. The results also show that while biomass of larger groups at the base of the food web (diatoms, copepods, and euphausiids) decreases during El Niño events, the smaller groups (flagellates and ciliates) thrive under the low-nutrient conditions. Furthermore, the eddy resolving resolution of the ROMS revealed that composite anomalies of NO_3 associated to El Niño and La Niña seem to follow meanderings of the CCS, and to be tightly related to spatially locked mesoscale features of the CCS. These interesting results will be topic of future research in order to clarify the relationships between the ecology and mesoscale eddy field of the CCS.

Acknowledgements

The model simulation (ROMS-NEMURO) used for this research was executed and generously provided by Dr. Enrique Curchitser and Dr. Raphael Dussin (Department of Environmental Sciences, Institute of Marine and Coastal Sciences, Rutgers University). The work presented in this chapter was facilitated by two CCE-LTER REU's from UCSD, Ms. Yunchun Pan (Applied Mathematics) and Mr. Lawrence Balitaan (Oceanic and Atmospheric Science). The results of Chapter 3 are currently being prepared for submission for publication, by Nathalí Cordero-Quirós, Arthur J. Miller, Yunchun Pan, Lawrence Balitaan, Raphael Dussin, and Enrique Curchitser. I also acknowledge Dr. Jerome Fiechter at University of California, Santa Cruz, for this helpful feedback and guidance in understanding the IBM. Prof. Chris Edwards provided extensive advice on the NEMURO model.

We are grateful to the National Science Foundation (California Current Ecosystem-LTER, OCE1637632, and Coastal SEES, OCE1600283) and the National Oceanic and

Atmospheric Administration (NOAA-MAPP; NA17OAR4310106) for funding that supported this research. N. Cordero-Quirós was partially supported by a UC Mexus CONACYT Fellowship.

References

Bograd, S.J., Pozo Buil, M., Du Lorenzo, E., Castro, C.G., Shroeder, I.D., Goericke, R., Andersson C.R., Benitez-Nelson, C., Whitney, F.A., 2015. Changes in source waters to the Southern California Bight. Deep Sea Res. 112, 42-52. https://doi.org/10.1016/j.dsr2.2014.04.009

Centurioni, L.R., Ohlmann,J.C., Niiler,P.P. 2008. Permanent meanders in the California Current System. J. Phys.Oceanogr. 38,1690–1710.

Cordero-Quirós, N., Miller, A.J., Subramanian A.C., Luo, J.Y., Capotondi, A., 2019. Composite physical-biological El Niño and La Niña conditions in the California Current System in CESM1-POP2-BEC. Ocean Modelling, 142, 101439. https://doi.org/10.1016/j.ocemod.2019.101439

Curchitser, E.N., Haidvogel, D.B., Hermann, A.J., Dobbins, E.L., Powell, T.M., Kaplan, A., 2005. Multi-scale modeling of the North Pacific Ocean: assessment and analysis of simulated basin-scale variability (1996–2003). J. Geophys. Res. 110. https://doi.org/10.1029/2005JC002902

Edwards, K.F., Thomas, M.K., Klausmeier, C.A., Litchman, E., 2012. Allometric scaling and taxonomic variation in nutrient utilization traits and maximum growth rate of phytoplankton. Limnol. Oceanogr. 57, 554–566. https://doi.org/10.4319/lo.2012.57.2.0554.

Fiechter, J., Rose, K. A., Curchitser, E. N., Hedstrom, K. S. 2015. The role of environmental controls in determining sardine and anchovy population cycles in the California Current: Analysis of an end-to-end model. Progress in Oceanography, 138, 381–398. https://doi.org/10.1016/j.pocean.2014.11.013

Fiedler, P.C., Mantua, N.J., 2017. How are warm and cool years in the California Current related to ENSO? J. Geophys. Res. Oceans 122 (7), 5936–5951. http://dx.doi.org/10.1002/2017JC013094.

Griffies, S., Biastoch, C., Bryan, F., Danabasoglu, G., Chassignet, E.P., England, M.H., Gerdes, R., Haak, H., Hallber, R.W., Hazeleger, W., Jungclaus, J., Large, W.G., Madec, F., Pirani, A., Samuels, B., Sheinert, M., Gupta, A.S., Severijns, C.A., Simmons, H.L., Treguier, A.M.,

Winton, M., Yeager, S., Yin, J., 2009. Coordinated ocean-ice reference experiments (CORE). Ocean Model. 26, 1–46.

Haidvogel, D.B., Arango, H., Budgell, W.P., Cornuelle, B.D., Curchitser, E., DiLorenzo, E., Fennel, K., Geyer, W.R., Hermann, A.J., Lanerolle, L., Levin, J., McWilliams, J.C., Miller, A.J., Moore, A.M., Powell, T.M., Shchepetkin, A.F., Sherwood, C.R., Signell, R.P., Warner, J.,C., Wilkin, J., 2008. Regional ocean forecasting in terrain- following coordinates: model formulation and skill assessment. J.Comput. Phys.227,3595–3624.

Kishi, M.J., Kashiwai, M., Ware, D.M., Megrey, B.A., Eslinger, D.L., Werner F.E., Noguchi-Aita, M., Azumaya, T., Fuji, ., Hashimoto, S., Huang, D., Izumi, H., Ishida, Y., Kang, S., Kantakov, G.A., Kim, H., Komatsu, K., Navrotsky, V.V., Smith, S.L., Tadokoro, K., Tsuda, A., Yamamura, O., Yamanaka, Y., Yokouchi, K., Yoshie, N., Zhang, J., Zuenko, Y.I., Zvalisnky, V.I. 2007. NEMURO—a lower trophic level model for the North Pacific marine ecosystem. Ecol. Model. 202, 12–25.

Marchesiello, P., McWilliams, J.C., Shchepetkin, A., 2003. Equilibrium structure and dynamics of the California Current system. Journal of Physical Oceanography 33 (4), 753–783.

McGowan, J.A., Cayan, D.R., Dorman, L.M., 1998. Climate-ocean variability and ecosystem response in the northeast Pacific. Science 281, 210–217.

Politikos, D.V., Curchitser, E.N., Rose, K.A., Checkley D.M., Fiechter, J., 2017. Climate variability and sardine recruitment in the California Current: A mechanistic analysis of an ecosystem model. Fisheries Oceanography 27, 602-622. DOI: 10.1111/fog.12381

Rayner, N.A., Parker, D.E., Horton, E.B., Folland, C.K., Alexander, L.V., Rowell, D.P., 2003. Global analyses of sea surface temperature, sea ice, and night marine air temperature since the late nineteenth century. J. Geophys. Res. 108, 4407. http://dx.doi.org/10.1029/2002JD002670.

Rose, K.A. et al., 2015. Demonstration of a fully-coupled end-to-end model for small pelagic fish using sardine and anchovy in the California Current. Progress in Oceanography 138 (PB), 348–380. http://dx.doi.org/10.1016/j.pocean.2015.01.012.

Rykaczewski, R.R., Dunne,J.P., 2010.Enhanced nutrient supply to the California Current Ecosystem with global warming and increased stratification in an earth system model. Geophys. Res. Lett.37, L21606, http://dx.doi.org/10.1029/ 2010GL045019.

Sánchez-Garrido, J., Fiechter, J., Rose, K., Werner, C., Curchitser, E. 2020. Dynamics of anchovy and sardine populations in the Canary Current off NW Africa: responses to environmental and climate forcing in a climate-to-fish ecosystem model. Fisheries in Oceanography. Under Revision.

Seo, H., A. J. Miller and J. R Norris, 2016: Eddy-wind interaction in the California Current System: Dynamics and impacts. *Journal of Physical Oceanography*, **46**, 439-459.

Shchepetkin, A.F., McWilliams,J .C., 2005.Theregional oceanic modeling system (ROMS): asplit-explicit, free-surface, topography-following-coordinate ocean model. OceanModel.9,347–404.

Stock, C.A., John, J.G., Rykaczewski, R.R., Asch, R.G., Cheung, W.W.L., Dunne, J.P., Friedland, K.D., Lam, V. W.Y., Sarmiento J.L., Watson R.A., 2017. Reconciling fisheries catch and ocean productivity. PNAS 114, E1441–E1449. https://doi.org/10.1073/pnas.1610238114.

Thomas, A.C., Strub, P.T., Weatherbee, R.A., James, C., 2012. Satellite views of Pacific chlorophyll variability: Comparisons to physical variability, local versus nonlocal influences and links to climate indices. Deep-Sea Res. II 77–80, 99–106.

Van Oostende, N., Dussin, R., Stock, C.A., Barton, A.D., Curchitser, E., Dunne, J.P., Ward, B.B., 2018. Simulating the ocean's chlorophyll dynamic range from coastal upwelling to oligotrophy. Progress in Oceanography 168, 232-247. https://doi.org/10.1016/j.pocean.2018.10.009

Chapter 4.

4.1 Summary and Prospects for Future Research

The focus of this dissertation is on understanding the California Current physical-biological response to ENSO variability. Since ENSO has potential for a predictive capacity, it is important to understand how useful this knowledge of future ENSO states could be for anticipating future ecological conditions in the CCS. The results described in Chapters 2 and 3 build on our present understanding of ecosystem predictability by using two widely-studied models to establish how confidently we can relate physical conditions associated with ENSO to consistent ecological changes in the CCS.

Chapter 2 considers the "climate-scale" response of the CCS and the CCE as captured by the coarse resolution global model, POP2-BEC, which is used in the NCAR CESM. In general, global circulation models have large biases in the EBUS regions derived partly from their inability to resolve coastal upwelling and mesoscale eddy effects, and the POP2-BEC is no exception. Despite the robust statistics of the large-scale CCS response where El Niño leads to predictable reductions in nutrients, and consequently phytoplankton and zooplankton biomass, the coarse resolution of the model produces a much weaker and less coherent response than observed, especially in the chlorophyll field. Additionally, the results of Chapter 2 shed light on a key feature of the composite response of the CCS to ENSO events: its asymmetry. Even though the most extreme events are associated with warming during El Niño (e.g., 97-98), La Niña events tend to drive a more consistently cool response in the SSTa of the CCS. This asymmetry is consequently also found in the modeled ecological fields.

Frontal regions of the EBUS are highly dominated by mesoscale features. In the CCS, the eddy field has an important role in transporting biogeochemical properties such as oxygen and chlorophyll. The effects of mesoscale eddies clearly cannot be resolved by a coarse resolution model, like POP2-BEC. Therefore, Chapter 3 uses a historical simulation of a highly-resolved "eddy-scale" model, the widely-used ROMS coupled to the NPZD ecosystem model NEMURO, to more accurately simulate and describe the mechanistic bottom-up response of the CCS and the CCE to ENSO events. The results neatly show how different phytoplankton and zooplankton groups respond differently to El Niño and La Niña events as a function of their size and physiology. This "El Niño winners and losers" characteristic is a noteworthy result of the analysis of this simulation with multiple classes of phytoplankton and zooplankton. The asymmetries of the ENSO-forced response occur in this model as well, especially for the larger components of the ecology.

Overall, these results motivate future research paths regarding the predictability of environmental conditions that modulate the CCS and predictability of its bottom-up ecosystem dynamics. For example, how sensitive is an ecosystem model to slight changes in the physical forcing? There are always uncertainties in the physical state of the CCS, and these uncertainties increase when making forecasts. An ecological model might behave very linearly in response to the physical drivers, so that small errors in the forcing might lead to small errors in the ecology. But if the ecological model is highly nonlinear, that may not be true and errors might be amplified by the nonlinear dynamics of ecology. This nonlinear ecological behavior can be quantified with a modeling strategy that addresses the predictable nature of the CCE by testing its sensitivity to changes in ecological initial conditions. Physical conditions can be specified

from a standard ROMS free run or from a data assimilated ROMS product (e.g, Crawford et al., 2018) and then used to force off-line simulations with the ecosystem model NEMURO. The initial states of NEMURO can then be slightly varied and an ensemble of ecological runs can establish if the ecology exhibits sensitivity to initial conditions. This will also allow to study how ecological fields develop in different regions of the CCS. For example, in the coastal region where forcing is strong, fast biological timescales are likely to rapidly adjust to the slow physical forcing, but the ecology may evolve differently in the offshore region dominated by eddies. Furthermore, creating this kind of ensemble of ecological simulations will allow to measure the predictable or chaotic nature of the ecosystem response to physical forcings derived from ENSO and other major climate oscillations.

As another example, what is the role of mesoscale features in the ENSO-related variability of the ecosystem? The daily physical fields of the ROMS driven with observed forcing can be analyzed to assess how the mesoscale eddies affect the evolution of the response of the CCS to ENSO variability. The eddy field may be modulated by the ENSO changes in the background conditions over the CCS, thereby affecting the nutrient fluxes controlling ecological productivity. An ensemble of physical model runs, with NEMURO, would be needed to conclusively address this effect in the ensemble-mean response for each ENSO event. This type of study will help to understand whether mesoscale features drive a coherent response of the biogeochemistry of the CCS on ENSO time scales, or if they simply obscure the predictability of the ecosystem by introducing random noise.

The focus of the two proposed experimental strategies described above is to shed light on the degree of predictability of the CCE that can be used in a practical forecasting sense on

seasonal to interannual timescales, as well as a climate projection sense as we transition into warmer global temperatures on decadal to centennial timescales. A solid scientific knowledge of the evolution of bottom-up dynamics of the ecosystem as driven by changes in the physical forcings is key to understand future changes in primary production and higher trophic levels. This can help understand how important commercial species such as sardine and anchovy may change their patterns and habitat for reproduction, migration, and feeding. All these issues are of extreme societal importance and are necessary to guide adequate management of fisheries along the U.S. West Coast.

Reference

Crawford, W., A. M. Moore, M. G. Jacox, J. Fiechter, E. Neveu, and C. A. Edwards (2018), A resonant response of the California Current circulation to forcing by low frequency climate variability, Deep Sea Research Part II, doi:10.1016/j.dsr2.2017.07.016.